

# Three-Body Recombination of Identical Bosons with a Large Positive Scattering Length at Nonzero Temperature

Eric Braaten,<sup>1,\*</sup> H.-W. Hammer,<sup>2,†</sup> Daekyoung Kang,<sup>1,‡</sup> and Lucas Platter<sup>1,3,§</sup>

<sup>1</sup>*Department of Physics, The Ohio State University, Columbus, OH 43210, USA*

<sup>2</sup>*Helmholtz-Institut für Strahlen- und Kernphysik (Theorie),  
Universität Bonn, 53115 Bonn, Germany*

<sup>3</sup>*Department of Physics and Astronomy,  
Ohio University, Athens, OH 45701, USA*

(Dated: February 25, 2019)

## Abstract

For identical bosons with a large scattering length, the dependence of the 3-body recombination rate on the collision energy is determined by universal functions of a single scaling variable. There are six scaling functions for angular momentum zero and one scaling function for each higher partial wave. We calculate these universal functions by solving the Skorniakov–Ter-Martirosian equation. The results for the 3-body recombination as a function of the collision energy are in good agreement with previous results from solving the 3-body Schrödinger equation for  $^4\text{He}$  atoms. The universal scaling functions can be used to calculate the 3-body recombination rate at nonzero temperature. We obtain an excellent fit to the data from the Innsbruck group for  $^{133}\text{Cs}$  atoms with a large positive scattering length.

PACS numbers: 21.45.-v, 34.50.-s, 03.75.Nt

Keywords: Few-body systems, three-body recombination, scattering of atoms and molecules.

---

\*Electronic address: braaten@mps.ohio-state.edu

†Electronic address: hammer@itkp.uni-bonn.de

‡Electronic address: kang@mps.ohio-state.edu

§Electronic address: platter.2@osu.edu

## I. INTRODUCTION

Three-body recombination is a 3-particle process in which two of the particles bind to form a molecule. This process is important in cold atom physics, because it is one of the most important loss mechanisms for trapped ultracold atoms. If the interactions of the atoms are known with sufficient accuracy, the 3-body recombination rate can be calculated by solving the 3-body Schrödinger equation numerically. However the interactions between complex atoms may not be known with sufficient accuracy. This is especially true for atoms whose S-wave scattering length  $a$  is large compared to their range. In this case, the atoms have *universal* properties that depend on  $a$  but are otherwise insensitive to length scales set by the range. This makes possible a complementary approach to the few-body problem that involves expanding in powers of the range divided by  $a$ . The leading term in this expansion is called the *zero-range limit* or, alternatively, the *scaling limit*. In the 3-body sector, the approach to the few-body problem based on expanding around the zero-range limit was pioneered by Vitaly Efimov beginning around 1970.

Efimov discovered that the zero-range limit of the 3-body problem for nonrelativistic particles with short-range interactions is quite remarkable. If  $a = \pm\infty$ , there are infinitely many 3-body bound states with an accumulation point at the 3-atom scattering threshold. These *Efimov states* or *Efimov trimers* have a geometric spectrum [1]:

$$E_T^{(n)} = (e^{-2\pi/s_0})^{n-n_*} \hbar^2 \kappa_*^2 / m, \quad (1)$$

where  $\kappa_*$  is the binding wavenumber of the Efimov trimer labeled by  $n_*$  and  $m$  is the mass of the particles. This geometric spectrum is a signature of a *discrete scaling symmetry* with discrete scaling factor  $e^{\pi/s_0}$  [2]. In the case of identical bosons,  $s_0 \approx 1.00624$  and the discrete scaling factor is  $e^{\pi/s_0} \approx 22.7$ . We will refer to the universal phenomena characterized by this discrete scaling symmetry as *Efimov physics* [3]. Efimov showed that discrete scale invariance is also relevant if  $a$  is large but finite [4, 5]. The negative values of  $a$  for which there is an Efimov trimer at the 3-atom scattering threshold are related by the discrete scaling symmetry. The positive values of  $a$  for which there is an Efimov trimer at the atom-dimer scattering threshold are also related by the discrete scaling symmetry. Another dramatic example of Efimov physics is the vanishing of the 3-body recombination rate at threshold at positive values of  $a$  that are related by the discrete scaling symmetry [6–8].

Efimov also showed that the discrete scaling symmetry governs the energy dependence of 3-body scattering processes, such as atom-dimer elastic scattering and 3-body recombination [5]. It is convenient to measure the total energy  $E$  of the three atoms in their center-of-mass frame relative to the 3-atom scattering threshold. The discrete scaling symmetry implies that the scattering rates at energy  $E$  in a system with parameters  $a$  and  $\kappa_*$  differ from those at energy  $(e^{-2\pi/s_0})^n E$  in a system with parameters  $(e^{\pi/s_0})^n a$  and  $\kappa_*$  only by an overall change in the scale. The zero-range limit gives more detailed predictions that Efimov referred to as the *Radial Law*. The Radial Law expresses the dependence of the scattering rates on  $E$  in terms of universal functions of a scaling variable  $x = (a^2 m E / \hbar^2)^{1/2}$ . Once these scaling functions have been calculated, the scattering rates can be predicted for any system of identical bosons with a large scattering length.

The universal results defined by the scaling limit are exact only in the limit of zero range. Corrections to the universal results associated with a nonzero range are suppressed by powers of  $\ell/|a|$ , where  $\ell$  is the natural low-energy length scale [2]. For a short-range potential,  $\ell$  is simply the range of the potential. For atoms whose potential has a van der Waals tail

$-C_6/r^6$ ,  $\ell$  is the van der Waals length  $\ell_{\text{vdW}} = (mC_6/\hbar^2)^{1/4}$ . The effects of the nonzero range can be calculated within a systematic expansion in the small parameter  $\ell/|a|$  [9–13]. The next-to-leading order term in this expansion is proportional to  $r_s/a$ , where  $r_s$  is the effective range [9, 10]. Surprisingly, the next-to-next-to-leading order term in this expansion is also determined only by the scattering length  $a$ , the Efimov parameter  $\kappa_*$ , and the effective range [13].

The natural low-energy length scale  $\ell$  allows us to differentiate between a *shallow dimer* and *deep dimers*. The shallow dimer is a universal feature of the two-body system with large positive scattering length and has binding energy  $E_D \approx \hbar^2/(ma^2)$ . The underlying interaction can also support deep dimers whose binding energies are comparable to or larger than  $\hbar^2/(m\ell^2)$ . The properties of these deep dimers are not universal. The alkali atoms used in most cold atom experiments form diatomic molecules with many deeply-bound energy levels. Efimov trimers can therefore decay into an atom and a deep dimer with large kinetic energies. These final states also provide inelastic atom-dimer scattering channels and additional 3-body recombination channels. If the atoms do not form deep dimers, the universal results for scattering rates are determined by two parameters: the scattering length  $a$  and the Efimov parameter  $\kappa_*$ . If the atoms do form deep dimers, the universal results for scattering rates are determined by three parameters:  $a$ ,  $\kappa_*$ , and a parameter  $\eta_*$  that determines the widths of the Efimov trimers [14, 15]. Remarkably, the same universal functions that determine the energy dependence of scattering rates for the case  $\eta_* = 0$  in which there are no deep dimers also determine their energy dependence for  $\eta_* > 0$ .

The first experimental evidence for Efimov physics was presented by the Innsbruck group [16]. They carried out experiments with ultracold  $^{133}\text{Cs}$  atoms in the lowest hyperfine state, using a magnetic field to control the scattering length. They observed a resonant enhancement in the 3-body recombination rate at  $a \approx -850 a_0$  that can be attributed to an Efimov trimer near the 3-atom threshold. At the temperature 10 nK, the loss rate as a function of  $a$  can be fit rather well by the universal formula for zero temperature derived in Ref. [15] with a width parameter  $\eta_* = 0.06(1)$ . The Innsbruck group also observed a local minimum in the 3-body recombination rate near  $a \approx 210 a_0$  that might be associated with an interference minimum of the 3-body recombination rate. The measurements were carried out at 200 nK, which is large enough that taking into account the nonzero temperature is essential.

The 3-body recombination rate can be calculated at nonzero temperature by carrying out a thermal average of the 3-body recombination rate as a function of the collision energy. There have been several previous calculations of the 3-body recombination rate for atoms with large scattering length at nonzero temperature using specific models. D’Incao, Suno, and Esry used a simple 2-parameter potential with either one or two S-wave bound states [17, 18]. Massignan and Stoof used a 4-parameter scattering model for atoms near a Feshbach resonance [19]. There have been several previous calculations of the 3-body recombination rate for nonzero temperature that have exploited the universality of atoms with large scattering length. In the case  $a < 0$ , the 3-body recombination rate was calculated by Jonsell using the adiabatic hyperspherical approximation [20] and by Yamashita, Frederico, and Tomio using a resonance approximation [21]. In the case  $a > 0$ , the 3-body recombination rate has been calculated using simplifying assumptions to neglect some of the universal scaling functions [22–24]. All these calculations involve uncontrolled approximations, so they

are not definitive predictions for large scattering length.<sup>1</sup>

In this paper, we present definitive universal predictions for the 3-body recombination rate at nonzero temperature for the case  $a > 0$ . We calculate the universal scaling functions that determine the hyperangular average of the 3-body recombination rate at collision energies up to about 30 times the binding energy of the shallow dimer. Our results are validated by comparing with a previous calculation of the 3-body recombination rate as a function of collision energy for  $^4\text{He}$  atoms. The universal scaling functions can be used to calculate the rate constants for 3-body recombination into the shallow dimer and into deep dimers at temperatures and densities where Boltzmann statistics are applicable. We apply the results to  $^{133}\text{Cs}$  atoms with large positive scattering length  $a$  and show that they give an excellent fit to the data from the Innsbruck group on the 3-body recombination rate as a function of  $a$ .

## II. THREE-BODY RECOMBINATION

Three-body recombination is a 3-atom collision process in which two of the atoms bind to form a diatomic molecule or *dimer*. We take the 3 atoms to have the same mass  $m$ . The 3-body recombination rate  $R(\mathbf{p}_1, \mathbf{p}_2, \mathbf{p}_3)$  is a function of the momenta of the three incoming atoms. Galilean invariance implies that  $R$  does not depend on the total momentum  $\mathbf{p}_{\text{tot}} = \mathbf{p}_1 + \mathbf{p}_2 + \mathbf{p}_3$ . It can therefore be expressed as a function  $R(\mathbf{p}_{12}, \mathbf{p}_{3,12})$  of a pair of Jacobi momenta  $\mathbf{p}_{12} = \mathbf{p}_1 - \mathbf{p}_2$  and  $\mathbf{p}_{3,12} = \mathbf{p}_3 - \frac{1}{2}(\mathbf{p}_1 + \mathbf{p}_2)$ . It is convenient to parameterize the Jacobi momenta in terms of 6 orthogonal variables: the collision energy  $E = (3p_{12}^2 + 4p_{3,12}^2)/(12m)$ , four Jacobi angles giving the orientations of the unit vectors  $\hat{\mathbf{p}}_{12}$  and  $\hat{\mathbf{p}}_{3,12}$ , and a hyperangle  $\alpha_3 = \arctan(\sqrt{3}p_{12}/(2p_{3,12}))$ . The integration element in these variables is

$$d^3p_1 d^3p_2 d^3p_3 = \sqrt{3} m^3 E^2 dE \sin^2(2\alpha_3) d\alpha_3 d\Omega_{12} d\Omega_{3,12} d^3p_{\text{tot}}. \quad (2)$$

We will refer to the average of a quantity over the Jacobi angles and over the hyperangle as the *hyperangular average*. We denote the hyperangular average of the 3-body recombination rate  $R(\mathbf{p}_{12}, \mathbf{p}_{3,12})$  by  $K(E)$ .

In a gas of atoms with number density  $n_A$ , the rate of decrease in the number density due to 3-body recombination defines an experimentally measurable loss rate constant  $L_3$ :

$$\frac{d}{dt}n_A = -L_3 n_A^3. \quad (3)$$

The event rate constant  $\alpha$  for 3-body recombination is defined so that the number of recombination events per time and per volume is  $\alpha n_A^3$ . If the number of atoms lost from the system per recombination event is  $n_{\text{lost}}$ , the rate constant is  $L_3 = n_{\text{lost}} \alpha$ . The binding energy of the dimer is released through the kinetic energies of the recoiling atom and dimer. If their kinetic energies are large enough that the atom and dimer both escape from the system and if the number density is low enough that subsequent collisions do not prevent them from escaping from the system, then  $n_{\text{lost}} = 3$ . On the other hand, if they both remain in the system and if we regard the dimer as a distinct chemical species with its own number density  $n_D$ , then  $n_{\text{lost}} = 2$ .

---

<sup>1</sup> Definitive universal predictions at temperatures small compared to the dimer binding energy are available for resonant dimer relaxation, which is an important loss process for atom-dimer mixtures [25].

In an ensemble of identical bosons with number density  $n_A$  in thermal equilibrium at temperature  $T$ , the event rate per volume and per time is  $\alpha n_A^3$ , where

$$\alpha(T) = \frac{\int R(\mathbf{p}_{12}, \mathbf{p}_{3,12}) n(E_1)n(E_2)n(E_3) d^3p_1 d^3p_2 d^3p_3}{3! \int n(E_1)n(E_2)n(E_3) d^3p_1 d^3p_2 d^3p_3} \quad (4)$$

and  $n(E)$  is the Bose-Einstein distribution:  $n(E) = [e^{(E-\mu)/(k_B T)} - 1]^{-1}$ . The chemical potential  $\mu$  is determined by the condition  $\int n(E_1) d^3p_1 / (2\pi)^3 = n_A$ . The factor of  $1/3!$  in Eq. (4) accounts for the indistinguishable nature of the three identical particles. The denominator in Eq. (4) can be written  $6 [\int n(E_1) d^3p_1]^3 = 6(2\pi)^9 n_A^3$ .

The critical temperature  $T_c$  for Bose-Einstein condensation is given by  $k_B T_c \approx 3.3 \hbar^2 n_A^{2/3} / m$ . If  $T$  is significantly larger than  $T_c$ , the product of the three Bose-Einstein distributions in Eq. (4) can be approximated by a Boltzmann distribution:

$$n(E_1)n(E_2)n(E_3) \approx e^{3\mu/(k_B T)} \exp(-E_{\text{tot}}/(k_B T)), \quad (5)$$

where  $E_{\text{tot}} = E_1 + E_2 + E_3$  is the total energy of the three atoms. The total energy can be expressed as the sum of the center-of-mass energy and the collision energy  $E$ :  $E_{\text{tot}} = p_{\text{tot}}^2/(6m) + E$ . The Gaussian integral over  $\mathbf{p}_{\text{tot}}$  cancels between the numerator and the denominator of Eq. (4). The effect of the integrals over the hyperangle and the Jacobi angles is to replace  $R(\mathbf{p}_{12}, \mathbf{p}_{3,12})$  in the numerator by its hyperangular average  $K(E)$ . Thus if  $T$  is significantly larger than  $T_c$ , the event rate constant  $\alpha(T)$  in Eq. (4) reduces to a Boltzmann average over the collision energy  $E$ :

$$\alpha(T) \approx \frac{\int_0^\infty dE E^2 e^{-E/(k_B T)} K(E)}{6 \int_0^\infty dE E^2 e^{-E/(k_B T)}}. \quad (6)$$

The integral in the denominator can be evaluated analytically to give  $2(k_B T)^3$ . We will refer to temperatures and densities for which this approximation is valid as the *Boltzmann region*. Note that the Boltzmann region can extend to arbitrarily low temperatures if the number density  $n_A$  is arbitrarily small. At  $T = 0$ , the approximation in Eq. (6) reduces to  $\alpha(0) = K(E = 0)/6$ . However this applies only if the temperature is small enough that  $K(E)$  can be approximated by  $K(0)$  but still in the Boltzmann region. At  $T = 0$ , the atoms are in a Bose-Einstein condensate. The correct result for the rate constant at  $T = 0$  is therefore  $\alpha(0) \approx K(E = 0)/36$ . The extra factor of  $1/3!$  comes from the 3 identical bosons being in the same quantum state.

If the scattering length  $a$  is positive and large compared to the range of the interaction, one of the dimers that can be produced by the recombination process is the shallow dimer. Its binding energy in the zero-range limit is

$$E_D = \hbar^2 / (ma^2). \quad (7)$$

If there are deep dimers, they can be produced by the recombination process for either sign of  $a$ . The recombination rate can be decomposed into the contribution from the shallow dimer and the sum of the contributions from all the deep dimers:

$$K(E) = K_{\text{shallow}}(E) + K_{\text{deep}}(E). \quad (8)$$

The 3-body recombination rate into the shallow dimer can be further decomposed into contributions from the channels in which the total orbital angular momentum of the three atoms has definite quantum number  $J$ :

$$K_{\text{shallow}}(E) = \sum_{J=0}^{\infty} K^{(J)}(E). \quad (9)$$

The threshold behavior for each of the angular momentum contributions to  $K_{\text{shallow}}(E)$  follows from a generalization of Wigner's threshold law [26]:  $K^{(J)}(E) \sim E^{\lambda_J}$ , where  $\lambda_0 = 0$ ,  $\lambda_1 = 3$ , and  $\lambda_J = J$  for  $J \geq 2$ . At the scattering threshold  $E = 0$ , only the  $J = 0$  term is nonzero.

The hyperangular average  $K_{\text{shallow}}(E)$  of the 3-body recombination rate is related in a simple way to the dimer-breakup cross section for the scattering of an atom and the shallow dimer:

$$K_{\text{shallow}}(E) = \frac{192\sqrt{3}\pi\hbar^3(E_D + E)}{m^2E^2}\sigma_{\text{breakup}}(E). \quad (10)$$

Thus in the Boltzmann region, the contribution to the event rate constant in Eq. (6) from 3-body recombination into the shallow dimer is determined by the dimer-breakup cross section  $\sigma_{\text{breakup}}(E)$ . Using the Optical Theorem,  $\sigma_{\text{breakup}}(E)$  can be determined from the phase shifts for elastic atom-dimer scattering. We will show in Section VI that in the case of a large scattering length,  $K_{\text{deep}}(E)$  is determined by the same universal functions that determine  $K_{\text{shallow}}(E)$ . Thus in the Boltzmann region, the rate constant for 3-body recombination is completely determined by the elastic atom-dimer scattering amplitude.

### III. UNIVERSAL SCALING BEHAVIOR

In this section, we consider atoms with a large positive scattering length and no deep dimers, so the only diatomic molecule is the shallow dimer whose binding energy is given by Eq. (7). The total 3-body recombination rate  $K(E)$  is therefore equal to  $K_{\text{shallow}}(E)$ , which is related to the dimer-breakup cross section by Eq. (10). We summarize the constraints of universality on the 3-body recombination rate for this case.

#### A. Angular momentum and hyperangular decompositions

The universal results for scattering rates, such as  $K_{\text{shallow}}(E)$ , are functions of the collision energy  $E$ , the scattering length  $a$ , and the Efimov parameter  $\kappa_*$  defined by Eq. (1). An alternative Efimov parameter that is particularly convenient when considering 3-body recombination is  $a_{*0}$ , which is one of the scattering lengths at which  $K_{\text{shallow}}(E)$  vanishes at  $E = 0$ . This Efimov parameter differs from  $\kappa_*^{-1}$  by a multiplicative factor that is known only to two digits of accuracy:

$$a_{*0} \approx 0.32 \kappa_*^{-1}. \quad (11)$$

The dependence of scattering rates on the Efimov parameter is strongly constrained by the discrete scale invariance. Their dependence on the energy  $E$  can be conveniently expressed in terms of universal functions of a dimensionless scaling variable  $x$  defined by

$$x = (ma^2E/\hbar^2)^{1/2}. \quad (12)$$

Atom-dimer scattering states in the center-of-mass frame can be labelled by the relative momentum  $\mathbf{k}$  between the atom and the dimer or, equivalently, by the energy  $E$  relative to the 3-atom threshold and the angular momentum quantum numbers  $J$  and  $M$ . The  $S$  matrix elements for atom-dimer elastic scattering are functions of  $E$  that are independent of  $M$  and diagonal in  $J$ . They can be expressed in terms of the phase shifts  $\delta_{AD}^{(J)}(E)$  for atom-dimer elastic scattering:

$$S_{AD,AD}^{(J)}(E) = e^{2i\delta_{AD}^{(J)}(E)}. \quad (13)$$

The phase shifts  $\delta_{AD}^{(J)}(E)$  are real below the 3-atom threshold and have a positive imaginary part for  $E > 0$ .

Three-atom scattering states in the center-of-mass frame can be labelled by the Jacobi momenta  $\mathbf{p}_{12}$  and  $\mathbf{p}_{3,12}$ . One can define subsystem angular momenta associated with rotations of the unit vectors  $\hat{\mathbf{p}}_{12}$  and  $\hat{\mathbf{p}}_{3,12}$ . We denote the associated angular momentum quantum numbers by  $\ell_x, m_x$  and by  $\ell_y, m_y$ , respectively. An equivalent set of quantum numbers are  $\ell_x, \ell_y$ , and the total orbital angular momentum quantum numbers  $J$  and  $M$ . The possible values of  $J$  are integers ranging from  $|\ell_x - \ell_y|$  to  $\ell_x + \ell_y$ . The range of the hyperangle  $\alpha_3$  is from 0 to  $\frac{1}{2}\pi$ . Since this range is compact, we can expand functions of  $\alpha_3$  in terms of orthogonal functions relative to the weight factor  $\sin^2(2\alpha_3)$  that are labelled by an index  $n_3 = 0, 1, 2, \dots$ . A convenient set of variables for the 3-atom scattering states is the collision energy  $E$  and five discrete variables:  $J, M, \ell_x, \ell_y$ , and the hyperangular index  $n_3$ . Since  $\ell_x, \ell_y$ , and  $n_3$  are a denumerable set, we will denote them collectively by a single integer  $n$  that takes values  $3, 4, 5, \dots$ . The reason for choosing this peculiar set of values will become clear in Section III C. The S-matrix elements for 3-body recombination can be expressed as functions  $S_{AAA,AD}^{(J,n)}(E)$  of the collision energy with index  $n$ . The contribution from angular momentum  $J$  to the hyperangular average of the 3-body recombination rate can be expressed as

$$K^{(J)}(E) = \frac{144\sqrt{3}\pi^2\hbar^5(2J+1)}{m^3E^2} \sum_{n=3}^{\infty} \left| S_{AAA,AD}^{(J,n)}(E) \right|^2. \quad (14)$$

The hyperangular average is implemented by the sum over  $n$ . The unitarity of the S-matrix in the angular momentum  $J$  sector implies

$$\left| S_{AD,AD}^{(J)}(E) \right|^2 + \sum_{n=3}^{\infty} \left| S_{AD,AAA}^{(J,n)}(E) \right|^2 = 1. \quad (15)$$

This can be used together with Eq. (13) to express the 3-body recombination rate in Eq. (14) in terms of the phase shifts  $\delta_{AD}^{(J)}(E)$  for elastic atom-dimer scattering:

$$K^{(J)}(E) = \frac{144\sqrt{3}\pi^2\hbar^5(2J+1)}{m^3E^2} \left( 1 - \left| e^{2i\delta_{AD}^{(J)}(E)} \right|^2 \right). \quad (16)$$

## B. Scaling behavior for $J \geq 1$

In the sector with angular momentum quantum number  $J \geq 1$ , the scattering rates do not depend on  $\kappa_*$ . The constraints of universality are therefore particularly simple for  $J \geq 1$ .

The atom-dimer phase shifts  $\delta_{AD}^{(J)}(E)$  defined by Eq. (13) are universal functions of the scaling variable  $x$  defined in Eq. (12). Below the 3-atom threshold, these scaling functions are real. Above the 3-atom threshold, they are complex.

The contribution to the 3-body recombination rate into the shallow dimer from angular momentum  $J$  has the form

$$K^{(J)}(E) = \frac{144\sqrt{3}\pi^2(2J+1)f_J(x)}{x^4} \frac{\hbar a^4}{m}, \quad (17)$$

where  $f_J(x)$  is a real-valued scaling function:

$$f_J(x) = 1 - \exp(-4 \operatorname{Im} \delta_{AD}^{(J)}(E)). \quad (18)$$

As  $x \rightarrow 0$ , the leading powers of  $x$  are determined by Wigner's threshold law [26]:  $f_J(x) \sim x^{2\lambda_J+4}$ , where  $\lambda_1 = 3$  and  $\lambda_J = J$  for  $J \geq 2$ .

### C. Discrete scaling behavior for $J = 0$

The universal results for  $J = 0$  are more intricate than for  $J \geq 1$ , because they depend not only on  $E$  and  $a$ , but also on  $\kappa_*$  or, equivalently,  $a_{*0}$ . General scaling formulas for scattering rates in the 3-atom sector can be derived from Efimov's Radial Law. The Radial Law expresses the S-matrix elements for low-energy scattering processes in the  $J = 0$  channel of the 3-atom sector in terms of universal functions of the scaling variable  $x$  defined in Eq. (12). The S-matrix elements for atom-dimer elastic scattering and for 3-body recombination from 3-atom states labelled ( $J = 0, n$ ) have the form

$$S_{AD,AD}^{(J=0)}(E) = s_{22}(x) + \frac{s_{21}(x)^2 e^{2i\theta_{*0}}}{1 - s_{11}(x) e^{2i\theta_{*0}}}, \quad (19a)$$

$$S_{AD,AAA}^{(J=0,n)}(E) = s_{2n}(x) + \frac{s_{21}(x) s_{1n}(x) e^{2i\theta_{*0}}}{1 - s_{11}(x) e^{2i\theta_{*0}}}, \quad (19b)$$

where the angle  $\theta_{*0}$  is

$$\theta_{*0} = s_0 \ln(a/a_{*0}). \quad (20)$$

The functions  $s_{ij}(x)$  are entries of an infinite-dimensional symmetric unitary matrix that depends only on the scaling variable  $x$  defined in Eq. (12). The unitarity of the infinite-dimensional matrix  $s$  can be expressed as

$$s_{1i}^* s_{1j} + s_{2i}^* s_{2j} + \sum_{n=3}^{\infty} s_{ni}^* s_{nj} = \delta_{ij}. \quad (21)$$

This condition implies the unitarity of the physical S-matrix for the  $J = 0$  sector. For example, one can use Eq. (21) to verify that the unitarity condition in Eq. (15) for  $J = 0$  is automatically satisfied if the S-matrix elements are given by the expressions in Eqs. (19).

Efimov's Radial Law has a simple interpretation in terms of the adiabatic hyperspherical representation of the 3-atom Schrödinger equation. The hyperradius  $R = [(r_{12}^2 + r_{23}^2 + r_{31}^2)/3]^{1/2}$  is the root-mean-square separation of the three atoms. We take the scattering length  $a$  to be much larger than the absolute value of the effective range  $r_s$ :  $a \gg |r_s|$ . In this case, there are four important regions of  $R$  for 3-atom configurations with energies near the scattering threshold:



- the *asymptotic* region  $R \gg a$ ,
- the *scaling* region  $R \sim a$ ,
- the *scale-invariant* region  $|r_s| \ll R \ll a$ ,
- the *short-distance* region  $R \sim |r_s|$ .

Efimov's radial law reflects the fact that there is only one adiabatic hyperspherical potential that is attractive in the scale-invariant region of  $R$ . It is only through this adiabatic hyperspherical potential that 3-atom configurations with energies near the scattering threshold can reach the short-distance region of  $R$ . The outgoing and incoming asymptotic states with respect to the scaling region are

1. incoming and outgoing hyperradial waves in the scale-invariant region  $|r_s| \ll R \ll a$  of the lowest adiabatic hyperspherical potential. We label these asymptotic states by the index 1.
2. outgoing or incoming atom-dimer scattering states with angular momentum quantum number  $J = 0$ . We label these asymptotic states  $AD$  or simply by the index 2.
3. outgoing or incoming 3-atom scattering states with  $J = 0$ . We label these asymptotic states  $AAA$  by the index  $n = 3, 4, 5, \dots$  that specifies  $\ell_x, \ell_y$ , and  $n_3$ .

The evolution of the 3-atom wavefunction through the scaling region is described by a unitary matrix  $s_{ij}$  whose indices correspond to the asymptotic states relative to the scaling region that were enumerated above. Time-reversal invariance implies that the matrix  $s$  is symmetric.

The expressions for the S-matrix elements in Eq. (19) have simple interpretations. The factor  $e^{2i\theta_{*0}}$  in Eqs. (19) is the phase shift due to reflection of a hyperradial wave from the short-distance region. The S-matrix elements in Eqs. (19) can be expanded as a power series in  $e^{2i\theta_{*0}}$  with each term corresponding to a different pathway between the incoming and outgoing scattering states. The term with the factor  $(e^{2i\theta_{*0}})^n$  is the amplitude for a pathway that includes  $n$  reflections from the short-distance region. In the S-matrix element  $S_{AD,AD}^{(J=0)}(E)$  in Eq. (19a), the leading term  $s_{22}$  is the amplitude for the incoming atom-dimer scattering state to be reflected from the scaling region. The second term  $s_{21}e^{2i\theta_{*0}}s_{12}$  is the amplitude for the atom-dimer scattering state to be transmitted through the scaling region to an incoming hyperradial wave, which is reflected from the short-distance region into an outgoing hyperradial wave, which is then transmitted through the scaling region to an outgoing atom-dimer scattering state. The factors of  $e^{2i\theta_{*0}}s_{11}$  from expanding the denominator are the amplitudes for the hyperradial wave to be reflected from the short-distance region and then reflected from the scaling region.

The contribution to the hyperangular average of the 3-body recombination rate from angular momentum  $J = 0$  can be obtained by using the unitarity condition in Eq. (15) to eliminate the sum over  $n$  in Eq. (14) and then inserting the expression for the S-matrix element in Eq. (19a):

$$K^{(0)}(E) = \frac{144\sqrt{3}\pi^2}{x^4} \left( 1 - \left| s_{22}(x) + \frac{s_{12}(x)^2 e^{2i\theta_{*0}}}{1 - s_{11}(x)e^{2i\theta_{*0}}} \right|^2 \right) \frac{\hbar a^4}{m}. \quad (22)$$

## D. Analytic results near threshold

Macek, Ovchinnikov, and Gasaneo have derived some remarkable analytic results for the 3-body problem of identical bosons with large scattering length and energies near the 3-atom threshold [27, 28]. In Ref. [27], they derived an analytic result for the S-wave phase shift  $\delta_{AD}^{(J=0)}(0)$  for atom-dimer elastic scattering at the breakup threshold  $E = 0$ . They obtained analytic results for the values  $s_{11}(0)$  and  $s_{12}(0)$  of the universal scaling functions at this threshold. In Ref. [28], they extended their analytic solution for  $\delta_{AD}^{(J=0)}(E)$  to the first nontrivial order in  $E$ . They used this result to derive an analytic expression for the 3-body recombination rate  $K_{\text{shallow}}(0)$  at the 3-atom threshold.

An analytic expression for the atom-dimer S-wave phase shift  $\delta_{AD}^{(0)}(E)$  near the dimer-breakup threshold is given in Ref. [28]. Using the first equality in Eq. (54) of Ref. [28] (to avoid typographical errors in the last line of Eq. (54)), the S-matrix element at energy  $E = x^2 E_D$  can be expressed in the form

$$\exp(2i\delta_{AD}^{(0)}(E)) = \frac{e^{2i[\delta_\infty(x) - \Delta(x)]}}{1 + e^{-2\pi s_0} e^{-2i\Delta(x)}} \left[ 1 + e^{-2\pi s_0} e^{2i\Delta(x)} + e^{-\pi s_0} A(x) (e^{2i\Delta(x)} - 1) \right], \quad (23)$$

where

$$\Delta(x) = \delta_0(x) - s_0 \ln(a/R_0). \quad (24)$$

The variable  $R_0$  is a matching point at short distances where the 3-body wavefunction vanishes. (The function  $\Delta(x)$  was denoted by  $\Delta(R_0)$  in Ref. [28].) The function  $A(x)$  and the energy dependent phases  $\delta_\infty(x)$  and  $\delta_0(x)$  are universal functions of the scaling variable  $x$ . By replacing the expression inside the absolute value signs in Eq. (22) by the phase shift in Eq. (23), the 3-body recombination rate can be expressed in the form

$$K^{(0)}(E) = 288\sqrt{3}\pi^2 \frac{A(x)}{x^4} \left( 1 - \frac{A(x)}{2\sinh(\pi s_0)} \right) \frac{\sinh(\pi s_0) \sin^2 \Delta(x)}{\sinh^2(\pi s_0) + \cos^2 \Delta(x)} \frac{\hbar a^4}{m}. \quad (25)$$

To determine the 3-body recombination rate at threshold, we need the limiting behavior of the functions  $A(x)$  and  $\delta_0(x)$  as  $x \rightarrow 0$ . The values of these phases at  $x = 0$  were calculated numerically in Ref. [27]:

$$\delta_\infty(0) = 1.736, \quad (26a)$$

$$\delta_0(0) = 1.588. \quad (26b)$$

The leading term in  $A(x)$  as  $x \rightarrow 0$ , which is proportional to  $x^4$ , was calculated analytically in Ref. [28]:

$$A(x) \rightarrow \frac{8(4\pi - 3\sqrt{3})}{3\sqrt{3}\sinh(\pi s_0)} x^4, \quad (27)$$

The recombination rate in Eq. (25) vanishes at the threshold if  $\Delta(0) = 0$ . Thus the expression for  $\Delta(x)$  in Eq. (24) can be written

$$\Delta(x) = \delta_0(x) - \delta_0(0) - s_0 \ln(a/a_{*0}), \quad (28)$$

where  $a_{*0}$  is a value of the scattering length for which the 3-body recombination rate vanishes at threshold. The expression for the S-wave atom-dimer phase shift in Eq. (23) reduces at the 3-atom threshold to

$$\delta_{AD}^{(0)}(E = 0) = \delta_\infty(0) + \arctan(\tanh(\pi s_0) \tan \theta_{*0}). \quad (29)$$

The expression given in Ref. [27] is equivalent but less compact. The analytic result of Macek, Ovchinnikov, and Gasaneo for the 3-body recombination rate at the 3-atom threshold [28] can be obtained by taking the limit  $x \rightarrow 0$  in Eq. (25):

$$K^{(0)}(E = 0) = \frac{768\pi^2(4\pi - 3\sqrt{3}) \sin^2[s_0 \ln(a/a_{*0})] \hbar a^4}{\sinh^2(\pi s_0) + \cos^2[s_0 \ln(a/a_{*0})] m}. \quad (30)$$

This result was also derived independently by Petrov [29]. For fixed  $a$ , the rate in Eq. (30) is a log-periodic function of  $a_{*0}$  that oscillates between zero and a maximum value

$$K_{\max} = 6C_{\max} \hbar a^4 / m, \quad (31)$$

where  $C_{\max}$  is

$$C_{\max} = \frac{128\pi^2(4\pi - 3\sqrt{3})}{\sinh^2(\pi s_0)}. \quad (32)$$

Its numerical value is  $C_{\max} \approx 67.1$ . The expression in Eq. (30) has zeroes when  $a$  is  $(e^{\pi/s_0})^n a_{*0}$ , where  $n$  is an integer. The maxima of  $K^{(0)}(0)$  in Eq. (33) occur when  $a$  is  $(e^{\pi/s_0})^n 14.3 a_{*0}$ . Since  $\sinh^2(\pi s_0) \approx 139$  is so large, the expression for  $K^{(0)}(0)$  in Eq. (30) can be approximated with an error of less than 1% of  $6C_{\max} \hbar a^4 / m$  by

$$K^{(0)}(E = 0) \approx 6C_{\max} \sin^2[s_0 \ln(a/a_{*0})] \hbar a^4 / m. \quad (33)$$

This approximate functional form of the rate constant was deduced independently in Refs. [6–8].

By comparing the expression for the S-matrix element in Eq. (23) with the Efimov's Radial Law in Eq. (19a), we can determine the universal scaling functions  $s_{11}(x)$ ,  $s_{12}(x)$ , and  $s_{22}(x)$  in the approximation of Ref. [28]:

$$s_{11}(x) \approx -e^{-2\pi s_0} e^{-2i[\delta_0(x) - \delta_0(0)]}, \quad (34a)$$

$$s_{12}(x) \approx e^{i[\delta_\infty(x) - \delta_0(x) + \delta_0(0)]} \sqrt{1 - e^{-4\pi s_0}} \left[ 1 - \frac{A(x)}{2 \sinh(\pi s_0)} \right]^{1/2}, \quad (34b)$$

$$s_{22}(x) \approx e^{2i\delta_\infty(x)} e^{-2\pi s_0} [1 + e^{\pi s_0} A(x)]. \quad (34c)$$

The limiting behavior of the functions  $\delta_\infty(x)$ ,  $\delta_0(x)$ , and  $A(x)$  as  $x \rightarrow 0$ , is given in Eqs. (26) and (27). At  $x = 0$ , we obtain  $s_{11}(0) = -e^{-2\pi s_0}$  and  $s_{12}(0) = e^{i\delta_\infty(0)} (1 - e^{-4\pi s_0})^{1/2}$ . These differ from the values deduced in Ref. [27] because a phase  $e^{2i\delta_0(0)}$  has been absorbed into  $e^{2i\theta_{*0}}$ . They also differ by a minus sign in  $s_{11}(0)$ . For small  $x$ , the leading terms in  $s_{12}(x) - s_{12}(0)$  and  $s_{22}(x) - s_{22}(0)$  scale like  $x^4$ . The leading terms in  $s_{11}(x) - s_{11}(0)$  scale like a higher power of  $x$ .

#### IV. UNIVERSAL SCALING FUNCTIONS

In this Section, we calculate the universal scaling functions associated with atom-dimer elastic scattering. These functions are then used to calculate the hyperangular average of the 3-body recombination rate as a function of the collision energy.

## A. STM Equation

Three-body observables for systems with a large scattering length can be calculated by solving an integral equation called the Skorniakov–Ter-Martirosian (STM) equation [30]. In momentum space, the STM equation can be expressed in the form [2]

$$\begin{aligned} \mathcal{A}(\mathbf{p}, \mathbf{k}; E) = & -\frac{16\pi/a}{mE - (p^2 + \mathbf{p} \cdot \mathbf{k} + k^2) + i\epsilon} \\ & - \int \frac{d^3q}{(2\pi)^3} \frac{8\pi}{mE - (p^2 + \mathbf{p} \cdot \mathbf{q} + q^2) + i\epsilon} \frac{\mathcal{A}(\mathbf{q}, \mathbf{k}; E)}{-1/a + \sqrt{-mE + 3q^2/4 - i\epsilon}}. \end{aligned} \quad (35)$$

The solution is, up to a normalization constant, the amplitude for an atom with momentum  $\mathbf{p}$  and energy  $p^2/(2m)$  and a pair of atoms with total momentum  $-\mathbf{p}$  and total energy  $E - p^2/(2m)$  to evolve into an atom with momentum  $\mathbf{k}$  and energy  $k^2/(2m)$  and a pair of atoms with total momentum  $-\mathbf{k}$  and total energy  $E - k^2/(2m)$ . The STM amplitude can be resolved into the contributions from channels with orbital angular momentum quantum number  $J$ :

$$\mathcal{A}_J(p, k; E) = \frac{1}{2} \int_{-1}^1 dx P_J(x) \mathcal{A}(\mathbf{p}, \mathbf{k}; E), \quad (36)$$

where  $x = \mathbf{p} \cdot \mathbf{k}/pk$  and  $P_J(x)$  is a Legendre polynomial.

In a specific angular momentum channel, the STM equation in Eq. (35) reduces to an integral equation with a single integration variable  $q$ . In the case  $J = 0$ , the behavior of the integral is sufficiently singular at large  $q$  that it is necessary to impose an ultraviolet cutoff  $q < \Lambda$ , where  $\Lambda$  is much greater than  $p$ ,  $k$  and  $(m|E|)^{1/2}$ . The STM equation for  $J = 0$  reduces to

$$\begin{aligned} \mathcal{A}_0(p, k; E, \Lambda) = & \frac{8\pi}{apk} \ln \frac{p^2 + pk + k^2 - mE - i\epsilon}{p^2 - pk + k^2 - mE - i\epsilon} \\ & + \frac{2}{\pi} \int_0^\Lambda dq \frac{q}{p} \ln \frac{p^2 + pq + q^2 - mE - i\epsilon}{p^2 - pq + q^2 - mE - i\epsilon} \frac{\mathcal{A}_0(q, k; E, \Lambda)}{-1/a + \sqrt{3q^2/4 - mE - i\epsilon}}. \end{aligned} \quad (37)$$

It can be shown that changing the ultraviolet cutoff  $\Lambda$  corresponds to changing the Efimov parameter  $\kappa_*$  [31–33]. The values of  $\Lambda$  and  $\kappa_*$  differ simply by a multiplicative constant:

$$\ln(\Lambda/\kappa_*) \approx 1.74 \pmod{(\pi/s_0)}. \quad (38)$$

The solutions of Eq. (37) are log-periodic functions of  $\Lambda$ . If  $\Lambda$  is increased by a factor of  $e^{\pi/s_0} \approx 22.7$ , it corresponds to the same value of  $\kappa_*$ . The S-wave atom-dimer phase shift  $\delta_{AD}^{(0)}(E)$  can be obtained from the amplitude with both momentum arguments  $p$  and  $k$  set equal to  $k_E = (\frac{4}{3}m(E_D + E))^{1/2}$ :

$$\mathcal{A}_0(k_E, k_E; E, \Lambda) = \frac{3\pi}{k_E \cot \delta_{AD}^{(0)}(E) - ik_E}. \quad (39)$$

This phase shift depends not only on the parameter  $a$  but also on the parameter  $\kappa_*$  through the dependence of the amplitude on  $\Lambda$ .

In the case  $J \geq 1$ , no ultraviolet cutoff is required and the partial wave projection of the STM equation leads to (see, e.g. Ref. [34])

$$\mathcal{A}_J(p, k; E) = \frac{16\pi}{apk} (-1)^J Q_J \left( \frac{p^2 + k^2 - mE - i\epsilon}{pk} \right) + \frac{4}{\pi} \int_0^\infty dq \frac{q}{p} Q_J \left( \frac{p^2 + q^2 - mE - i\epsilon}{pq} \right) \frac{(-1)^J \mathcal{A}_J(q, k; E)}{-1/a + \sqrt{3q^2/4 - mE - i\epsilon}}, \quad (40)$$

where

$$Q_J(z) = \frac{1}{2} \int_{-1}^1 dx \frac{P_J(x)}{z - x} \quad (41)$$

is a Legendre function of the second kind. The atom-dimer phase shift  $\delta_{AD}^{(J)}(E)$  can be obtained from

$$\mathcal{A}_J(k_E, k_E; E) = \frac{3\pi}{k_E \cot \delta_{AD}^{(J)}(E) - ik_E}, \quad \text{for } J \geq 1. \quad (42)$$

This phase shift is a function of the dimensionless variable  $ma^2E/\hbar^2$ .

### B. Universal scaling functions for $J \geq 1$

We calculate the atom-dimer phase shifts  $\delta_{AD}^{(J)}(E)$  for  $J = 1, 2, \dots, 6$  as functions of the energy  $E$  from  $10^{-2}E_D$  to  $10^2E_D$ . The scaling variable  $x$  defined in Eq. (12) then ranges from 0.1 to 10. For each energy  $E$ , we solve the STM equation in Eq. (40) and determine the phase shift  $\delta_{AD}^{(J)}(E)$  using Eq. (39). The universal scaling function  $f_J(x)$  defined in Eq. (18) is then determined from the imaginary part of the phase shift. Our numerical method loses accuracy for  $x$  smaller than values that range from 0.1 for  $J = 2$  to  $x = 0.45$  for  $J = 6$ . To determine  $f_J(x)$  for smaller values of  $x$ , we fit our results for the lowest 10 accurate points to the form

$$f_J(x) = a_J x^{2\lambda_J+4} + b_J x^{2\lambda_J+6}. \quad (43)$$

The exponent  $\lambda_J$  is predicted by Wigner's threshold law [26]:  $\lambda_1 = 3$  and  $\lambda_J = J$  for  $J \geq 2$ . We use the formula in Eq. (43) to extrapolate to small values of  $x$  where our numerical method loses accuracy. Our results are shown in Fig. 1. For  $J \geq 2$ ,  $f_J(x)$  is a decreasing function of  $J$ . This pattern is broken by  $f_1(x)$ , which is smaller than  $f_2(x)$  and  $f_3(x)$  at small  $x$  but eventually becomes larger than  $f_2(x)$  around  $x = 9$ .

### C. Universal scaling functions for $J = 0$

We calculate the atom-dimer phase shift  $\delta_{AD}^{(0)}(E)$  by solving the STM equation for  $J = 0$  with an ultraviolet cutoff  $\Lambda$ , which is given in Eq. (37), for energies  $E$  ranging from  $10^{-2}E_D$  to  $10^2E_D$ . We choose values of the ultraviolet cutoff  $\Lambda$  that are equally spaced on a log scale and cover three quarters of a discrete scaling cycle from  $\Lambda_0$  to  $10.4\Lambda_0$ . The smallest cutoff  $\Lambda_0$  is chosen to be much greater than  $1/a$  and  $(m|E|/\hbar^2)^{1/2}$ . For each energy  $E$ , we calculate the phase shift as a function of  $\log(a\Lambda)$  and fit it to the universal formula

$$\exp \left( 2i\delta_{AD}^{(J=0)}(E) \right) = s_{22}(x) + \frac{s_{12}(x)^2 \exp[2is_0 \ln(a/a_{*0})]}{1 - s_{11}(x) \exp[2is_0 \ln(a/a_{*0})]} \quad (44)$$

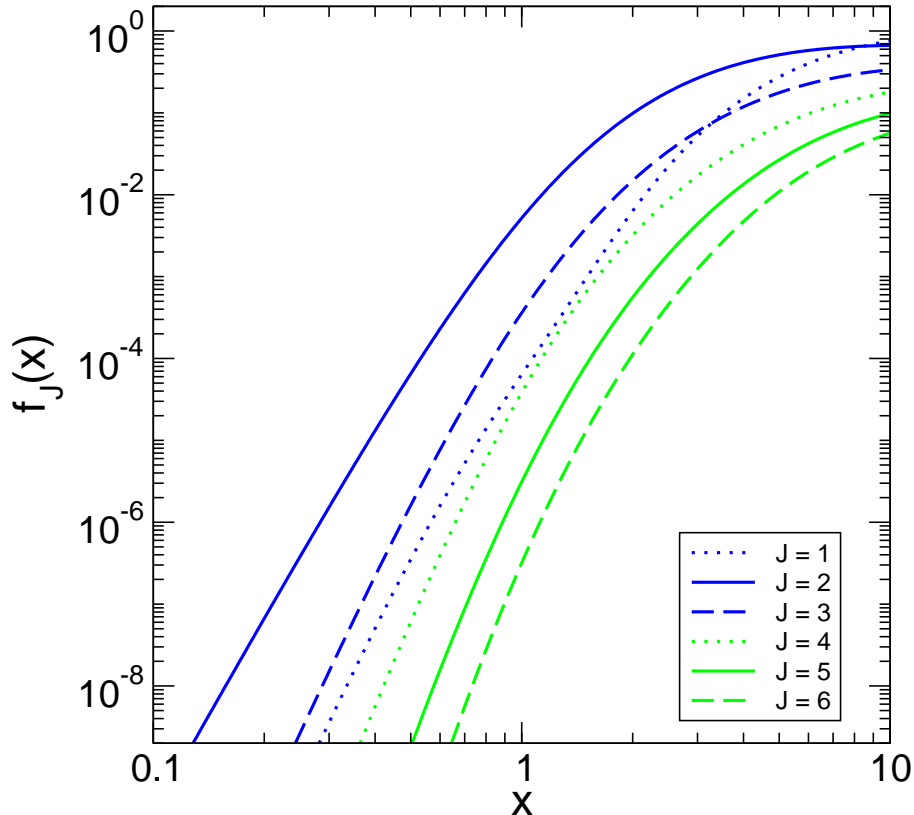


FIG. 1: The universal scaling functions  $f_J(x) = 1 - \exp(-4\text{Im}\delta_{AD}^{(J)}(E))$  for  $J = 1, \dots, 6$  as functions of the scaling variable  $x$ .

to determine the universal scaling functions  $s_{12}(x)$ ,  $s_{22}(x)$ , and  $s_{11}(x)$ . The sign ambiguity in  $s_{12}(x)$  is resolved by using continuity together with the analytic result for  $s_{12}(0)$  given by Eq. (34b).

The numerical results for the modulus  $|s_{ij}(x)|$  and the phase  $\arg s_{ij}(x)$  of each of these functions are shown in Fig. 2. The modulus  $|s_{12}(x)|$  remains close to 1 for  $x < 1$  but it decreases to 0.59 at  $x = 10$ . The moduli  $|s_{11}(x)|$  and  $|s_{22}(x)|$  both have the tiny value 0.0018 at  $x = 0$  and they remain tiny for  $x < 1$ . While  $|s_{22}(x)|$  increases to 0.37 at  $x = 10$ ,  $|s_{11}(x)|$  increases much more slowly to 0.035.

#### D. Three-body recombination rates

In this subsection, we use the universal scaling functions calculated in the previous sections to calculate the 3-body recombination rate into the shallow dimer. We show the contributions from angular momentum  $J = 0$  through 6 as functions of the collision energy.

In Eq. (22), the  $J = 0$  contribution  $K^{(0)}(E)$  to the 3-body recombination rate is expressed in terms of the universal scaling functions  $s_{11}(x)$ ,  $s_{12}(x)$ , and  $s_{22}(x)$ . In Fig. 3, it is shown as a function of the collision energy  $E$  for 6 values of  $\theta_{*0}$ :  $0$ ,  $\frac{1}{30}\pi$ ,  $\frac{1}{10}\pi$ ,  $\frac{1}{2}\pi$ ,  $\frac{9}{10}\pi$ , and  $\frac{29}{30}\pi$ . For  $\theta_{*0} = \frac{1}{2}\pi$ ,  $K^{(0)}(E)$  at  $E = 0$  has the maximum possible value  $K_{\max}$  given in Eq. (31) and it decreases monotonically with  $E$ . For  $\theta_{*0} = 0$  or  $\pi$ ,  $K^{(0)}(E)$  vanishes at  $E = 0$ , increases to a maximum value of  $0.0143 K_{\max}$  at  $E = 4.61 E_D$ , and then decreases. For  $\theta_{*0}$  between  $\frac{1}{2}\pi$

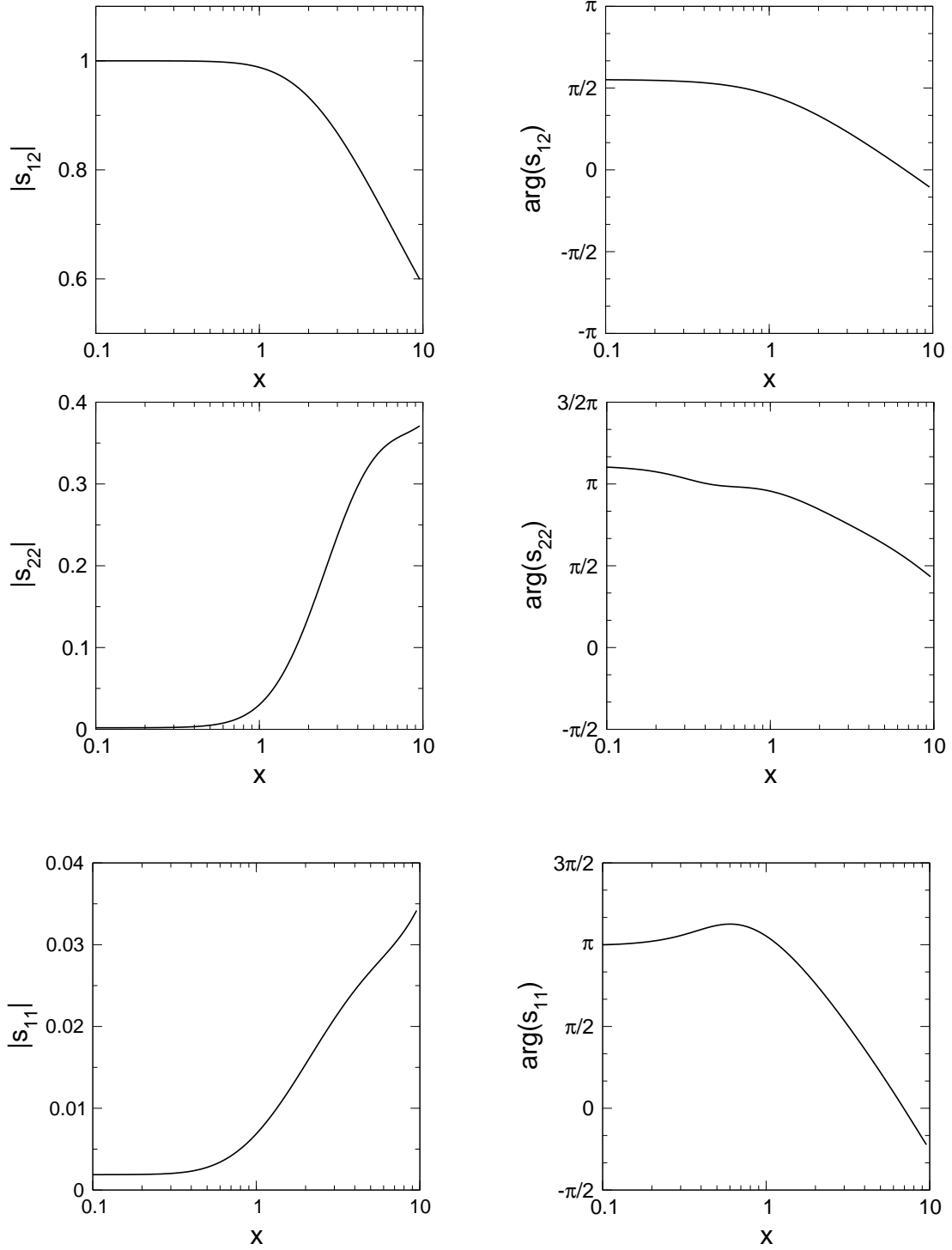


FIG. 2: The universal scaling functions  $s_{12}(x)$  (upper panels),  $s_{22}(x)$  (middle panels), and  $s_{11}(x)$  (lower panels) as functions of  $x$ . The modulus  $|s_{ij}(x)|$  and the phase  $\arg s_{ij}(x)$  of the function are shown in the left panel and the right panel, respectively.

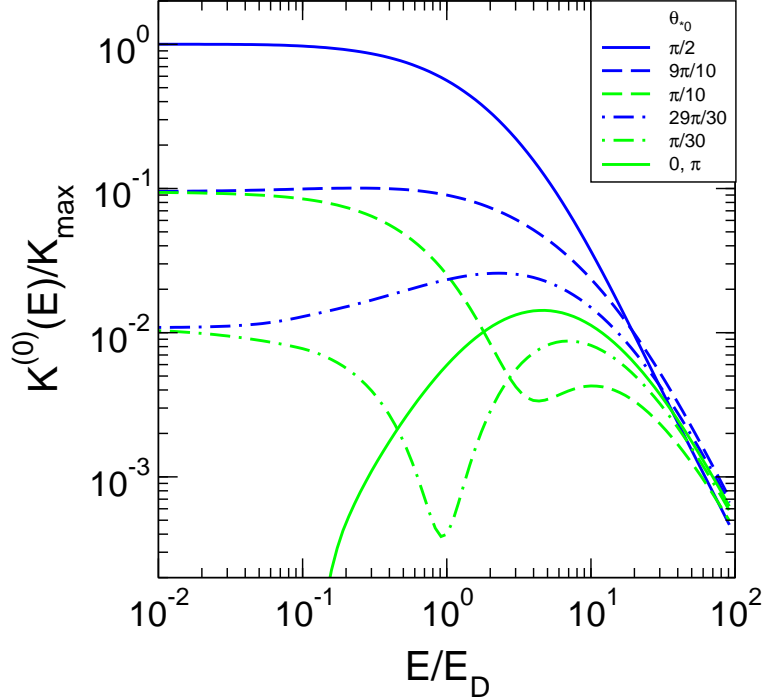


FIG. 3: (Color online) The  $J = 0$  contribution to the 3-body recombination rate into the shallow dimer for the case in which there are no deep dimers. The hyperangular average  $K^{(0)}(E)$  is shown as a function of the collision energy  $E$  for 6 values of  $\theta_{*0}$ :  $\frac{1}{2}\pi$  (upper solid line),  $\frac{9}{10}\pi$  and  $\frac{1}{10}\pi$  (upper and lower dashed lines),  $\frac{29}{30}\pi$  and  $\frac{1}{30}\pi$  (upper and lower dash-dotted lines), 0 or  $\pi$  (lower solid line).

and  $\pi$ ,  $K^{(0)}(E)$  has its maximum at a nonzero energy. As  $\theta_{*0}$  increases from  $\frac{1}{2}\pi$  to  $\pi$ , the local minimum at  $E = 0$  becomes increasingly deep and the maximum moves outward from 0 to  $4.61 E_D$ . For  $\theta_{*0}$  between 0 and  $0.124\pi$ ,  $K^{(0)}(E)$  has a local minimum at a nonzero energy  $E$ . As  $\theta_{*0}$  increases from 0 to  $0.124\pi$ , the local minimum moves outward from 0 to about  $8 E_D$  and its depth decreases until it becomes just an inflection point. For  $\theta_{*0}$  between  $0.124\pi$  and  $\frac{1}{2}\pi$ ,  $K^{(0)}(E)$  decreases monotonically with  $E$ .

At small energies, the dimensionless recombination rate  $K^{(0)}(E)/K_{\max}$  varies by many orders of magnitude as  $a_{*0}$  ranges over a complete discrete scaling cycle. Even at  $E = E_D$ , it varies by more than 3 orders of magnitude. The variations with  $a_{*0}$  become smaller at larger energy. If there were no relevant length scales at high energy, dimensional analysis would imply that  $K^{(0)}(E)$  should be proportional to  $E^{-2}$  at large  $E$ . Our results at the largest values of  $E$  are compatible with the approach to this simple scaling behavior. The differences between  $K^{(0)}(E)$  for different values of  $a_{*0}$  seem to decrease as a higher power of  $E$ . Our results at the largest values of  $E$  are compatible with their approach to the asymptotic behavior  $E^{-5/2}$ .

In Eq. (17), the contribution  $K^{(J)}(E)$  to the 3-body recombination rate from angular momentum  $J$  is expressed in terms of the universal scaling functions  $f_J(x)$ . In Fig. 4, the rates  $K^{(J)}(E)$  for  $J$  from 1 to 6 are shown as functions of the collision energy  $E$ . Over the range from 0 to  $100 E_D$ , the largest of these contributions is the  $J = 2$  term. It reaches its



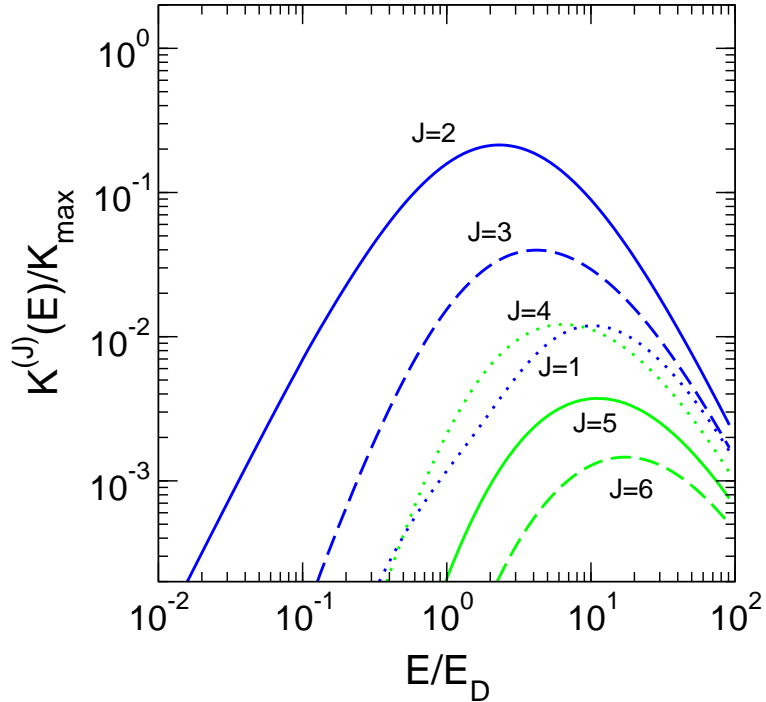


FIG. 4: (Color online) The contributions to the 3-body recombination rate into the shallow dimer from angular momenta  $J = 1, \dots, 6$ . The hyperangular averages  $K^{(J)}(E)$  are shown as a function of the collision energy  $E$ .

maximum value of  $0.214 K_{\max}$  at  $E = 4.18 E_D$ . The total contribution from  $J = 1, 3, 4, 5$ , and  $6$  is less than 10% of the  $J = 2$  contribution if  $E < 0.78 E_D$ . Thus the sum of the terms for  $J = 0$  and  $2$  is a good approximation to the recombination rate if  $E < 0.78 E_D$ . The sum of the contributions from  $J = 5$  and  $6$  is less than 10% of the sum of the contribution from  $J = 1$  through  $4$  if  $E < 32 E_D$ . Thus the sum of the terms for  $J = 0$  through  $4$  is a good approximation to the recombination rate if  $E < 32 E_D$ . Truncations of the partial wave expansion quickly become inaccurate at higher energies.

## V. APPLICATION TO $^4\text{He}$ ATOMS

The results from the previous section can be applied directly to systems of  $^4\text{He}$  atoms.<sup>2</sup> There are several modern potentials that are believed to describe the interactions of  $^4\text{He}$  atoms with low energy accurately. They all support a single weakly-bound diatomic molecule (or dimer). The effective ranges for all these potentials are approximately  $r_s \approx 14 a_0$ , which is a little larger than the van der Waals length scale  $(mC_6/\hbar^2)^{1/4} = 10.2 a_0$ . The scattering lengths are larger by about a factor of ten, and they vary among the potentials. The large scattering length,  $a \gg r_s$ , implies that  $^4\text{He}$  atoms have universal properties

<sup>2</sup> A convenient conversion constant for  $^4\text{He}$  atoms is  $\hbar^2/m = 43.2788 \text{ K } a_0^2$ .

that are determined by  $a$  and the Efimov parameter  $\kappa_*$ . First-order range corrections to the universal results are estimated to be suppressed by roughly  $r_s/a$  if  $E \lesssim E_D$  and by  $r_s(mE/\hbar^2)^{1/2} = xr_s/a$  for  $E \gtrsim E_D$ . This makes  $^4\text{He}$  atoms an ideal system to illustrate the universal properties of atoms with large scattering length. A thorough analysis of the universal properties of  $^4\text{He}$  atoms has been presented by Braaten and Hammer [35]. Various 3-body observables for  $^4\text{He}$  atoms have been calculated by Platter and Phillips to next-to-next-to-leading order in the expansion in powers of  $r_s/a$  [13]. The agreement with numerical results from exact solutions of the 3-body Schrödinger equation [36, 37] is impressive.

The 3-body recombination rate for  $^4\text{He}$  atoms was first calculated by Suno, Esry, Greene, and Burke [38]. They solved the 3-body Schrödinger equation for  $^4\text{He}$  atoms interacting through the HFD-B3-FCI1 potential [39]. They calculated  $K_{\text{shallow}}(E)$  as a function of the collision energy from the threshold to 10 mK [38], including the contributions with angular momentum quantum number  $J = 0, 1, 2$ , and 3. Their results are shown as dots in Fig. 5. Shepard has calculated the 3-body recombination rates of  $^4\text{He}$  atoms for the HFD-B3-FCI1 and other  $^4\text{He}$  potentials using separable potentials that reproduce the corresponding two-body phase shifts together with a 3-body force that is adjusted to fit the binding energy of the excited trimer [23].

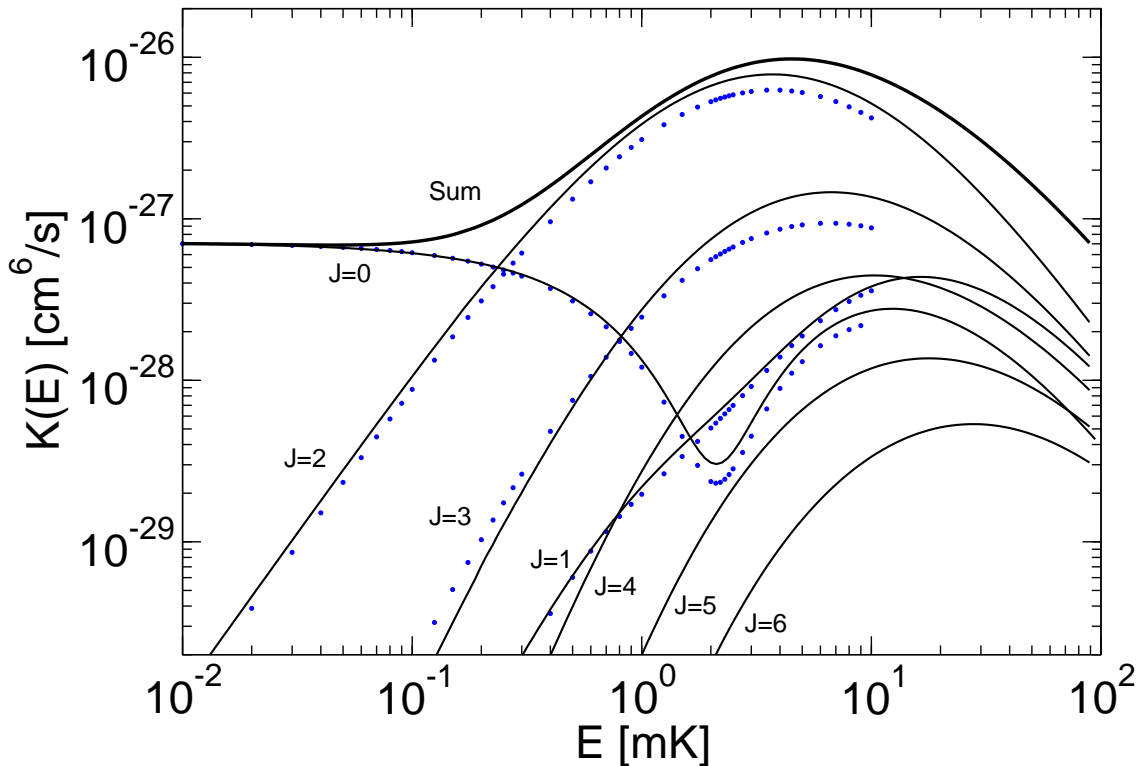


FIG. 5: (Color online) The 3-body recombination rates  $K^{(J)}(E)$  for  $^4\text{He}$  atoms (in units of  $\text{cm}^6/\text{s}$ ) as functions of the collision energy  $E$  (in units of mK) for  $J = 0$  through 6. The solid lines are our universal results for  $a = 164.5 a_0$  and  $a_{*0} = 143.1 a_0$ . The dots are the results obtained in Ref. [38] by solving the 3-body Schrödinger equation for the HFD-B3-FCI1 potential.

To apply the universal predictions for the 3-body recombination rate to  $^4\text{He}$  atoms interacting through the HFD-B3-FCI1 potential, we must determine the scattering length  $a$  and the 3-body parameter  $a_{*0}$  for that potential. The scattering length for the HFD-B3-FCI1

potential is  $a = 172 a_0$  and the binding energy of the shallow dimer is  $E_D = 1.600$  mK [40]. The universal predictions for low-energy 3-body observables are most accurate if the dimer bound state pole is at the correct position [35]. Therefore, we use the dimer binding energy as the 2-body input instead of  $a$ . Using the universal expression for the dimer binding energy in Eq. (7), we obtain the scattering length

$$a^{\text{He}} = 164.5 a_0. \quad (45)$$

We can determine the value of  $a_{*0}$  for  $^4\text{He}$  atoms interacting through the HFD-B3-FCI1 potential from the value of the 3-body recombination loss rate at threshold:  $K_{\text{shallow}}(0) = 7.10 \times 10^{-28}$  cm<sup>6</sup>/s. Inserting  $a^{\text{He}} = 164.5 a_0$  in Eq. (30) and solving for  $a_{*0}$ , we obtain

$$a_{*0}^{\text{He}} = 143.1 a_0. \quad (46)$$

The result for  $a_{*0}^{\text{He}}$  is approximately equal to  $0.870 a^{\text{He}}$ . The near equality between  $a_{*0}^{\text{He}}$  and  $a^{\text{He}}$  reflects the fact that  $K_{\text{shallow}}(0)$  for  $^4\text{He}$  is much smaller than the maximum value  $6C_{\text{max}}\hbar(a^{\text{He}})^4/m = 3.67 \times 10^{-26}$  cm<sup>6</sup>/s allowed by universality, which implies that  $a/a_{*0}$  is close to a zero of the sine function in the numerator of Eq. (30). The value of  $a_{*0}$  for  $^4\text{He}$  can also be determined from the binding energy of the excited  $^4\text{He}$  trimer, which is  $E_3^{(1)} = 2.62$  mK for the HFD-B3-FCI1 potential [40]. The resulting value,  $a_{*0} \approx 146 a_0$ , is consistent with the value in Eq. (46). Its accuracy is limited by the accuracy to which the numerical value of the constant in Eq. (11) is known.

The universal predictions for  $K^{(J)}(E)$  are given in Eq. (22) for  $J = 0$  and in Eq. (17) for  $J \geq 1$ . The only information about the HFD-B3-FCI1 potential that we use are the values of  $a$  and  $a_{*0}$  given in Eqs. (45) and (46). Our results for  $K^{(J)}(E)$ ,  $J = 0, 1, \dots, 6$ , are shown as solid lines in Fig. 5. The  $J = 0$  term dominates at low energies, but has a dramatic dip near 2 mK, where it is smaller than its value at  $E = 0$  by about a factor of 30. The  $J = 2$  term takes over as the dominant term when the energy exceeds about 0.2 mK. When it reaches its maximum value at an energy near 4 mK, other partial waves begin to give important contributions.

Our results can be compared with those of Ref. [38] for  $J = 0, 1, 2$ , and 3, which are shown as dots in Fig. 5. The qualitative agreement is excellent. The deep local minimum for  $J = 0$  and the peculiar shape for  $J = 1$  are both reproduced by the universal results. There is also good quantitative agreement for  $J = 0, 1$ , and 2. At  $E = E_D = 1.6$  mK, the fractional discrepancies for  $J = 0, 1$ , and 2 are 18.5%, 14.4%, and 20.3%, respectively. This is a little larger than the expected fractional error from range corrections, which is  $r_s/a = 8.5\%$ . At  $E = 10$  mK, which is the highest energy for which the 3-body recombination rate was calculated in Ref. [38], the fractional discrepancies for  $J = 0, 1$ , and 2 are 16.5%, 6.0%, and 18.6%. They are consistent with the expected fractional error from range corrections, which is  $xr_s/a = 21\%$ . For  $J = 3$ , the agreement between our results and those of Ref. [38] is not as good. The fractional discrepancy varies from +77% at 0.1 mK to -36% at 10 mK. Shepard has also calculated the contributions to the 3-body recombination rate for the HFD-B3-FCI1 potential from partial waves up to  $J = 3$  [23]. His results for  $J = 3$  are similar to ours and show the same discrepancy with Ref. [38]. The agreement between our results for  $J = 3$  and those of Ref. [23] gives us confidence in the accuracy of our numerical calculations. We do not understand the origin of the discrepancy with the results of Ref. [38].

The inclusion of higher order corrections in  $r_s/a$  should improve the agreement with the results of Ref. [38] at all energies. If the first order corrections in  $r_s/a$  are included, the errors

should decrease to roughly  $(r_s/a)^2 = 0.7\%$  for  $E \lesssim E_D = 1.6$  mK and to roughly  $(xr_s/a)^2$  at higher energies. A first calculation of the range corrections to the threshold recombination rate  $K_{\text{shallow}}(0)$  was carried out in Ref. [41].

## VI. EFFECTS OF DEEP DIMERS

In this section and in the subsequent section, we consider atoms that have deep dimers. In the scaling (or zero-range) limit, the cumulative effect of all the deep dimers on Efimov physics can be taken into account through one additional parameter  $\eta_*$  [15]. The atom-dimer phase shift and the hyperangular average of the 3-body recombination rate are determined by the same universal scaling functions as for  $\eta_* = 0$ .

### A. Generalization of Efimov's Radial Law

The existence of deep dimers implies that there are states in the 3-atom sector with energies near the 3-atom threshold that consist of an atom and a deep dimer with large kinetic energies. We will denote these states by the symbol  $\mathbf{AD}$ . These states provide inelastic atom-dimer scattering channels and additional 3-body recombination channels. In the scaling limit, the only contributions to the recombination rate into deep dimers are from the  $J = 0$  channels. The contributions from  $J \geq 1$  are suppressed by powers of  $r_s/a$ . The hyperangular average of the inclusive 3-body recombination rate into deep dimers can be expressed as

$$K_{\text{deep}}(E) = \frac{144\sqrt{3}\pi^2\hbar^5}{m^3E^2} \sum_{n=3}^{\infty} \sum_{\mathbf{AD}} \left| S_{\mathbf{AAA},\mathbf{AD}}^{(J=0,n)}(E) \right|^2, \quad (47)$$

where  $S_{\mathbf{AAA},\mathbf{AD}}^{(J=0,n)}(E)$  is the S-matrix element for the transition from a 3-atom scattering state labelled by  $(J = 0, n)$  to a specific state  $\mathbf{AD}$  consisting of an atom and deep dimer. The hyperangular average is implemented in Eq. (47) by the sum over  $n$ .

The states  $\mathbf{AD}$  also have an effect on the amplitudes for atom-dimer elastic scattering and for 3-body recombination into the shallow dimer. These effects are strongly constrained by the fact that the states  $\mathbf{AD}$  can be accessed only through a single adiabatic hyperspherical channel: the  $J = 0$  channel whose potential is attractive in the scale-invariant region of the hyperradius  $R$ . If there are deep dimers, an incoming hyperradial wave need not be totally reflected from the short-distance region of  $R$ , because it can ultimately emerge as a scattering state consisting of an atom and a deep dimer. The reflected hyperradial wave will therefore differ from the incident hyperradial wave not only by a phase shift  $e^{2i\theta_{*0}}$  but also by a decrease in its amplitude by a factor  $e^{-2\eta_*}$ . The parameter  $\eta_*$ , which was introduced in Ref. [14], determines the widths of Efimov trimers as well as all other effects of the deep dimers on low-energy 3-atom scattering processes. If the universal expression for an amplitude for the case of no deep dimers is known as an analytic function of  $a_{*0}$ , the corresponding result for a system with deep dimers can be obtained without any additional calculation simply by making the substitution

$$\ln a_{*0} \longrightarrow \ln a_{*0} - i\eta_*/s_0. \quad (48)$$

The generalization of Efimov's Radial Laws in Eqs. (19) to the case of atoms with deep

dimers are

$$S_{AD,AD}^{(J=0)}(E) = s_{22}(x) + \frac{s_{21}(x)^2 e^{2i\theta_{*0} - 2\eta_*}}{1 - s_{11}(x)e^{2i\theta_{*0} - 2\eta_*}}, \quad (49a)$$

$$S_{AD,AAA}^{(J=0,n)}(E) = s_{2n}(x) + \frac{s_{21}(x)s_{1n}(x)e^{2i\theta_{*0} - 2\eta_*}}{1 - s_{11}(x)e^{2i\theta_{*0} - 2\eta_*}}. \quad (49b)$$

Thus these S-matrix elements are determined by the same universal scaling functions  $s_{ij}(x)$  as in the case  $\eta_* = 0$  with no deep dimers.

The S-matrix elements for transitions from an atom-dimer scattering state or from a 3-atom scattering state into a specific state  $AD$  consisting of an atom and a deep dimer depend on details of physics at short distances. However as pointed out in Refs. [14, 15], the inclusive probability summed over all such states  $AD$  is insensitive to short distances and is determined completely by the parameters  $a$ ,  $\kappa_*$  and  $\eta_*$ . The inclusive probabilities for producing an atom and a deep dimer from an atom-dimer collision or from the collision of three atoms in the state labelled  $(J = 0, n)$  are

$$\sum_{AD} |S_{AD,AD}^{(J=0)}(E)|^2 = \frac{(1 - e^{-4\eta_*})|s_{21}(x)|^2}{|1 - s_{11}(x)e^{2i\theta_{*0} - 2\eta_*}|^2}, \quad (50a)$$

$$\sum_{AD} |S_{AAA,AD}^{(J=0,n)}(E)|^2 = \frac{(1 - e^{-4\eta_*})|s_{n1}(x)|^2}{|1 - s_{11}(x)e^{2i\theta_{*0} - 2\eta_*}|^2}. \quad (50b)$$

The factor  $s_{21}$  in Eq. (50a) is the amplitude for an incoming atom-dimer scattering state to be transmitted through the scaling region into a hyperradial wave in the scale-invariant region. The factor  $1/(1 - s_{11}e^{2i\theta_{*0} - 2\eta_*})$  takes into account an arbitrary number of reflections of the hyperradial wave from the short-distance region and then from the scaling region. The factor  $1 - e^{-4\eta_*}$  is the probability that a hyperradial wave incident on the short-distance region will not be reflected and will therefore ultimately emerge as a scattering state of an atom and a deep dimer. The analog of the unitarity condition in Eq. (15) for the case  $\eta_* > 0$  is

$$|S_{AD,AD}^{(J=0)}(E)|^2 + \sum_{n=3}^{\infty} |S_{AD,AAA}^{(J=0,n)}(E)|^2 + \sum_{AD} |S_{AD,AD}^{(J=0)}(E)|^2 = 1. \quad (51)$$

If we insert the S-matrix elements in Eqs. (49) and the probability in Eq. (50a), we can use the unitarity conditions for the matrix  $s_{ij}$  in Eq. (21) to show that Eq. (51) is automatically satisfied.

The hyperangular average of the 3-body recombination rate into the shallow dimer is obtained by squaring the S-matrix element in Eq. (49b), summing over the index  $n$  labelling the 3-atom states, and then multiplying by a kinematic factor. Using the unitarity condition in Eq. (51), the expression for the S-matrix element in Eq. (49a), and the expression for the probability in Eq. (50a), this can be expressed as

$$K^{(0)}(E) = \frac{144\sqrt{3}\pi^2}{x^4} \left( 1 - \left| s_{22}(x) + \frac{s_{12}(x)^2 e^{2i\theta_{*0} - 2\eta_*}}{1 - s_{11}(x)e^{2i\theta_{*0} - 2\eta_*}} \right|^2 - \frac{(1 - e^{-4\eta_*})|s_{12}(x)|^2}{|1 - s_{11}(x)e^{2i\theta_{*0} - 2\eta_*}|^2} \right) \frac{\hbar a^4}{m}. \quad (52)$$

This reduces to Eq. (22) in the limit  $\eta_* \rightarrow 0$ . The hyperangular average of the inclusive 3-atom recombination rate into deep dimers is given by summing the probability in Eq. (50b)

over the index  $n$  labelling the 3-atom states and then multiplying by a kinematic factor. Using the unitarity of the matrix  $s_{ij}(x)$ , the rate can be expressed as

$$K_{\text{deep}}(E) = \frac{144\sqrt{3}\pi^2(1 - e^{-4\eta_*})(1 - |s_{11}(x)|^2 - |s_{12}(x)|^2)}{x^4|1 - s_{11}(x)e^{2i\theta_{*0}-2\eta_*}|^2} \frac{\hbar a^4}{m}. \quad (53)$$

This contribution vanishes in the limit  $\eta_* \rightarrow 0$ . The recombination rates in Eqs. (52) and (53) are completely determined by the same universal scaling functions  $s_{11}(x)$ ,  $s_{12}(x)$ , and  $s_{22}(x)$  that determine the 3-body recombination rate into shallow dimers in the case  $\eta_* = 0$ .

## B. Analytic results at threshold

Analytic expressions for the 3-body recombination rates  $K_{\text{shallow}}(0) = K^{(0)}(0)$  and  $K_{\text{deep}}(0)$  at the threshold  $E = 0$  can be obtained by inserting the analytic results for the universal scaling functions  $s_{11}(x)$ ,  $s_{12}(x)$ , and  $s_{22}(x)$  in Eqs. (34) into Eqs. (52) and (53). The 3-body recombination rates at threshold into the shallow dimer and into deep dimers are

$$K_{\text{shallow}}(0) = \frac{768\pi^2(4\pi - 3\sqrt{3})(\sin^2[s_0 \ln(a/a_{*0})] + \sinh^2 \eta_*)}{\sinh^2(\pi s_0 + \eta_*) + \cos^2[s_0 \ln(a/a_{*0})]} \frac{\hbar a^4}{m}, \quad (54a)$$

$$K_{\text{deep}}(0) = \frac{384\pi^2(4\pi - 3\sqrt{3}) \coth(\pi s_0) \sinh(2\eta_*)}{\sinh^2(\pi s_0 + \eta_*) + \cos^2[s_0 \ln(a/a_{*0})]} \frac{\hbar a^4}{m}. \quad (54b)$$

Since  $\sinh^2(\pi s_0 + \eta_*) > 139$  is so large, these expressions can be approximated with errors of less than 1% by omitting the  $\cos^2$  terms in the denominators. To within the same accuracy, we can approximate  $\sinh(\pi s_0 + \eta_*)$ ,  $\sinh(\pi s_0)$ , and  $\cosh(\pi s_0)$  by exponentials to get the simpler expressions

$$K_{\text{shallow}}(0) \approx 6C_{\text{max}}e^{-2\eta_*} (\sin^2[s_0 \ln(a/a_{*0})] + \sinh^2 \eta_*) \hbar a^4/m, \quad (55a)$$

$$K_{\text{deep}}(0) \approx \frac{3}{2}C_{\text{max}}(1 - e^{-4\eta_*}) \hbar a^4/m, \quad (55b)$$

where  $C_{\text{max}} \approx 67.1$  is given in Eq. (32).

## C. Three-body recombination rate

In this subsection, we use the universal scaling functions calculated in the previous section to calculate the 3-body recombination rate into deep dimers and the  $J = 0$  contribution to the 3-body recombination rate into the shallow dimer. The effects of deep dimers on the contributions to the 3-body recombination rate into the shallow dimer from  $J \geq 1$  are suppressed in the zero-range limit.

In Eq. (52), the  $J = 0$  contribution  $K^{(0)}(E)$  to the 3-body recombination rate into the shallow dimer is expressed in terms of the universal scaling functions  $s_{11}(x)$ ,  $s_{12}(x)$ , and  $s_{22}(x)$ . In Fig. 6, it is shown as a function of the collision energy  $E$  for 6 values of  $\theta_{*0}$ : 0,  $\frac{1}{30}\pi$ ,  $\frac{1}{10}\pi$ ,  $\frac{1}{2}\pi$ ,  $\frac{9}{10}\pi$ , and  $\frac{29}{30}\pi$ . The left and right panels are for  $\eta_{*0} = 0.1$  and 0.2, respectively. Comparing with Fig. 3 for  $\eta_{*0} = 0$ , we see that the local minimum for  $\theta_{*0}$  between 0 and  $0.124 a_0$  becomes less pronounced as  $\eta_*$  increases. When  $\eta_*$  is large enough, the local

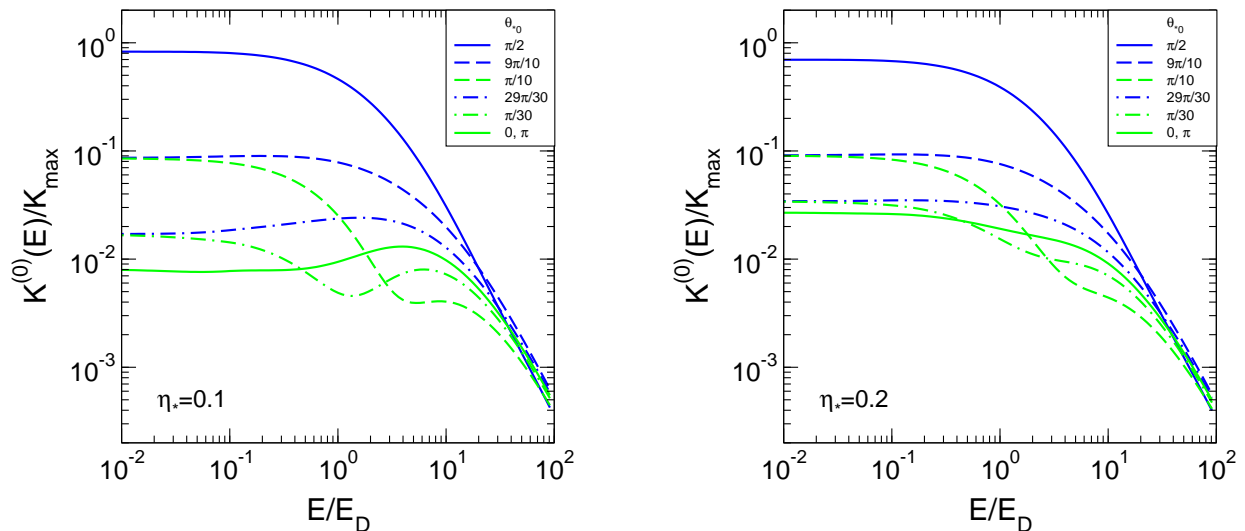


FIG. 6: (Color online) The  $J = 0$  contribution to the 3-body recombination rate into the shallow dimer for cases in which there are one or more deep dimers. The hyperangular average  $K^{(0)}(E)$  is shown as a function of the collision energy  $E$  or 6 values of  $\theta_{*0}$ :  $\frac{1}{2}\pi$  (upper solid line),  $\frac{9}{10}\pi$  and  $\frac{1}{10}\pi$  (upper and lower dashed lines),  $\frac{29}{30}\pi$  and  $\frac{1}{30}\pi$  (upper and lower dash-dotted lines),  $0, \pi$  (lower solid line). The left and right panels are for  $\eta_* = 0.1$  and  $\eta_* = 0.2$ , respectively.

minimum disappears altogether and  $K^{(0)}(E)$  becomes a monotonically decreasing function of  $E$ .

In Eq. (53), the 3-body recombination rate into deep dimers is expressed in terms of the universal scaling functions  $s_{11}(x)$  and  $s_{12}(x)$ . In Fig. 7, the maximum and minimum values of  $K_{\text{deep}}(E)$  with respect to variations of  $\theta_{*0}$  are shown for three values of  $\eta_{*0}$ : 0.01, 0.1, and 0.2. The differences between the maximum and minimum values are only visible at energies greater than  $E_D$ . The 3-body recombination rate into deep dimers is insensitive to the value of  $\theta_{*0}$ , because the dependence on  $\theta_{*0}$  in Eq. (53) is suppressed by a factor of  $s_{11}(x)$ , which remains small for  $x < 10$ . For any value of  $\eta_*$ ,  $K_{\text{deep}}(E)$  decreases monotonically with  $E$ . If there were no relevant length scales at high energy, dimensional analysis would imply that  $K_{\text{deep}}(E)$  should be proportional to  $E^{-2}$  at large  $E$ . Our results at the largest values of  $E$  are compatible with the approach to this simple scaling behavior.

## VII. APPLICATION TO $^{133}\text{CS}$ ATOMS

The Innsbruck group has carried out measurements of the 3-body recombination rate for ultracold  $^{133}\text{Cs}$  atoms<sup>3</sup> in the  $|f = 3, m_f = +3\rangle$  hyperfine state [16]. By varying the magnetic field from 0 to 150 G, they were able to change the scattering length from  $-2500 a_0$  through 0 to  $+1600 a_0$ . In this range of magnetic field, the  $|f = 3, m_f = +3\rangle$  state is the lowest hyperfine state, so 2-body losses are energetically forbidden. Thus, the dominant

<sup>3</sup> A convenient conversion constant for  $^{133}\text{Cs}$  atoms is  $\hbar^2/m = 1.30339 \text{ K } a_0^2$ .

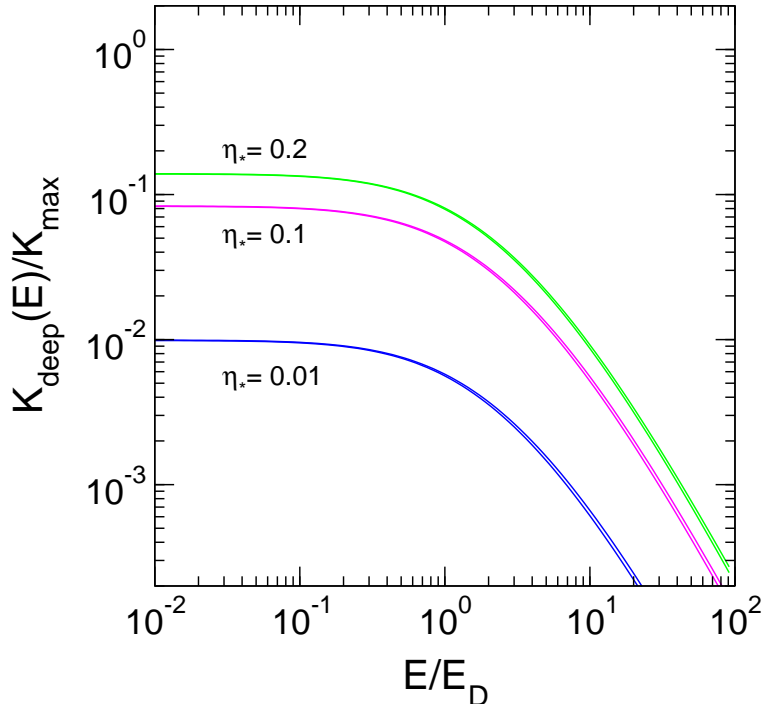


FIG. 7: (Color online) Three-body recombination rate into deep dimers. The maximum and minimum values of  $K_{\text{deep}}(E)$  with respect to variations of  $\theta_{*0}$  are shown as functions of the collision energy  $E$  for three values of  $\eta_*$ : 0.01, 0.1, and 0.2.

loss mechanism is 3-body recombination. The van der Waals length scale for Cs atoms is  $(mC_6/\hbar^2)^{1/4} \approx 200a_0$ . The range of scattering lengths studied by the Innsbruck group includes a universal region of large negative  $a$  and a universal region of large positive  $a$  separated by a nonuniversal region of small  $|a|$ . In the two regions of large scattering length, few-body physics should be universal and characterized by 3-body parameters  $\kappa_*$  and  $\eta_*$  that may be different in each universal region. An interesting open question is whether there is any relation between the 3-body parameters  $\kappa_*$  and  $\eta_*$  for different universal regions.

In the region of negative  $a$ , the Innsbruck group measured the loss rate constant  $L_3$  as a function of  $a$  at three different temperatures:  $T = 10$  nK, 200 nK, and 250 nK. They observed a dramatic enhancement of the loss rate for  $a$  near  $-850 a_0$ . At  $T = 10$  nK, the loss rate as a function of  $a$  can be fit rather well by the universal formula for  $T = 0$  in Ref. [15] with parameters  $a'_* = -850(20) a_0$  and  $\eta_* = 0.06(1)$ , where  $a'_*$  denotes the negative scattering length for which there is an Efimov resonance at the 3-atom threshold. Thus, the large enhancement in the loss rate can be explained by the resonant enhancement from an Efimov trimer near the 3-atom threshold. More recently, the Innsbruck group has measured the position of the maximum loss rate as a function of the temperature [42]. Its behavior as a function of temperature can be explained at least qualitatively by the dependence of the binding energy and width of the Efimov resonance on the scattering length [20, 21].

In the region of positive  $a$ , the Innsbruck group measured the loss rate constant  $L_3$  at  $T = 200$  nK for values of  $a$  ranging from  $62.3 a_0$  to  $1228 a_0$ . Their results in this region are



shown in Fig. 8. The vertical axis is the recombination length  $\rho_3$  defined by

$$\rho_3 = \left( \frac{2m}{\sqrt{3}\hbar} L_3 \right)^{1/4}. \quad (56)$$

They observed a local minimum in the loss rate for  $a$  near  $200 a_0$ . This value is near the van der Waals length scale  $(mC_6/\hbar^2)^{1/4} \approx 200 a_0$ , so range corrections may be large near the minimum. The universal prediction for the loss rate at  $T = 0$  is  $\alpha = K(0)/6$ , where  $K(0)$  is the sum of  $K_{\text{shallow}}(0)$  and  $K_{\text{deep}}(0)$  in Eqs. (54). To an approximation of better than 1%, they can be approximated by the expressions in Eqs. (55). By fitting the data for  $a > 500 a_0$  to this expression, they obtained  $a_+ = 1060(70) a_0$  for the scattering length  $e^{\pi/(2s_0)} a_{*0}$  at which the coefficient of  $a^4$  achieves its maximum value. Universality would then imply that the minimum should be at  $a_{*0} = 223(15) a_0$ . The fit was insensitive to the value of  $\eta_*$  and yielded only the upper bound  $\eta_* < 0.2$ . The Innsbruck group also determined the location of the minimum directly by measuring the fraction of atoms that were lost after a fixed time. The result was  $a_{\text{min}} = 210(10) a_0$ , which is consistent with the value obtained by fitting the data for  $a > 500 a_0$ .

We now consider whether our results can be applied to this system of  $^{133}\text{Cs}$  atoms. In the experiments with positive scattering length, the typical peak number density was  $5 \times 10^{13} \text{ cm}^{-3}$ . The corresponding critical temperature for Bose-Einstein condensation is  $T_c \approx 160 \text{ nK}$ . Thus, the temperature  $T = 200 \text{ nK}$  was not far above  $T_c$ . We ignore this complication and calculate thermal averages using the Maxwell-Boltzmann distribution as in Eq. (6) instead of the Bose-Einstein distribution. When  $a = a_{\text{min}}$ , the universal prediction for the binding energy  $E_D$  of the shallow dimer in Eq. (7) gives  $3 \times 10^4 \text{ nK}$ , so  $T/E_D \approx 0.007$ . The binding energy  $E_D$  decreases to about  $9 \times 10^2 \text{ nK}$  at  $a = 1228 a_0$ , so  $T/E_D \approx 0.22$ . Thus the temperature  $T = 200 \text{ nK}$  is safely in the region  $T < 30 E_D$  in which the thermal average in Eq. (6) can be calculated accurately using the scaling functions calculated in Section IV.

In Fig. 8, we compare the universal predictions for the recombination length  $\rho_3$  defined in Eq. (56) with the Innsbruck data for  $T = 200 \text{ nK}$  in the  $a > 0$  region. A blow-up of the region  $0 < a < 400 a_0$  is shown in the left panel of Fig. 9. We assume  $n_{\text{lost}} = 3$ , so that  $L_3 = 3\alpha$ . We set  $a_{*0} = 210 a_0$ , which is the central value of  $a_{\text{min}}$  measured in the Innsbruck experiment. In Fig. 8, we plot  $\rho_3$  as a function of  $a$  for  $T = 200 \text{ nK}$  and three values of  $\eta_*$ : 0, 0.1 and 0.2. The predictions for nonzero  $\eta_*$  are larger than those for  $\eta_* = 0$  in the region  $a < 500 a_0$  and smaller in the region  $a > 500 a_0$ . We extend the universal predictions down to  $a = 100 a_0$ , which is smaller than the effective range of Cs atoms, even though range corrections are expected to be 100% at such small values of  $a$ . The predictions for  $\eta_* = 0$  give a good fit to the data only in the region near  $500 a_0$  where the predictions are insensitive to  $\eta_*$ . The prediction for  $\eta_* = 0.2$  gives a remarkably good fit to the data for  $a$  ranging from the highest point at  $1228 a_0$  all the way down to  $202.7 a_0$ . As  $a$  decreases below  $200 a_0$ , the prediction for  $\eta_* = 0.2$  continues to decrease monotonically while the data seems to have a local maximum near  $137.3 a_0$ . The best fit to the data for  $a$  in the range from  $202.7 a_0$  to  $1228 a_0$  is  $\eta_* = 0.18$ , which gives a  $\chi^2$  per data point of 1.22.

In the right panel of Fig. 9, we show the universal prediction for the lower temperature of  $T = 40 \text{ nK}$ . For  $\eta_* = 0$ , the local minimal of  $\rho_3$  at  $210 a_0$  becomes much deeper at  $40 \text{ nK}$ . The predictions for  $\eta_* = 0.1$  and  $\eta_* = 0.2$  at  $40 \text{ nK}$  are essentially indistinguishable from the predictions at  $200 \text{ nK}$  in the region  $a < 600 a_0$ .

In Fig. 10, we illustrate the temperature dependence of the recombination length. We show  $\rho_3$  for  $\eta_* = 0.2$  as a function of  $a$  for three temperatures: 0, 40 nK, and 200 nK.

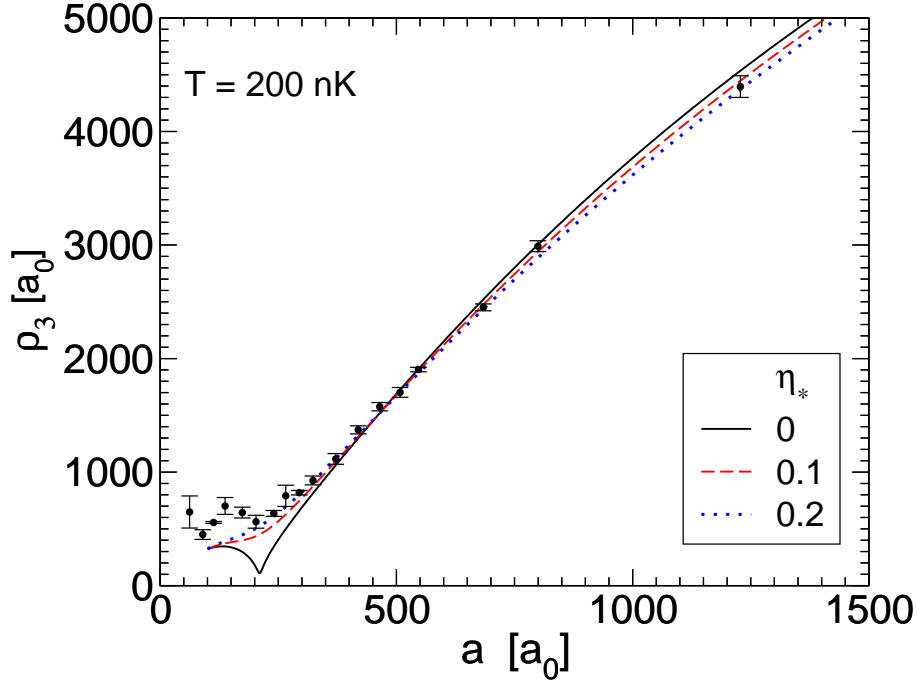


FIG. 8: (Color online) The 3-body recombination length  $\rho_3$  for  $^{133}\text{Cs}$  atoms as a function of  $a$  for  $T = 200$  nK. The data points are from Ref. [16]. The curves are the universal prediction for three values of  $\eta_*$ : 0 (solid line), 0.1 (dashed line), and 0.2 (dotted line).

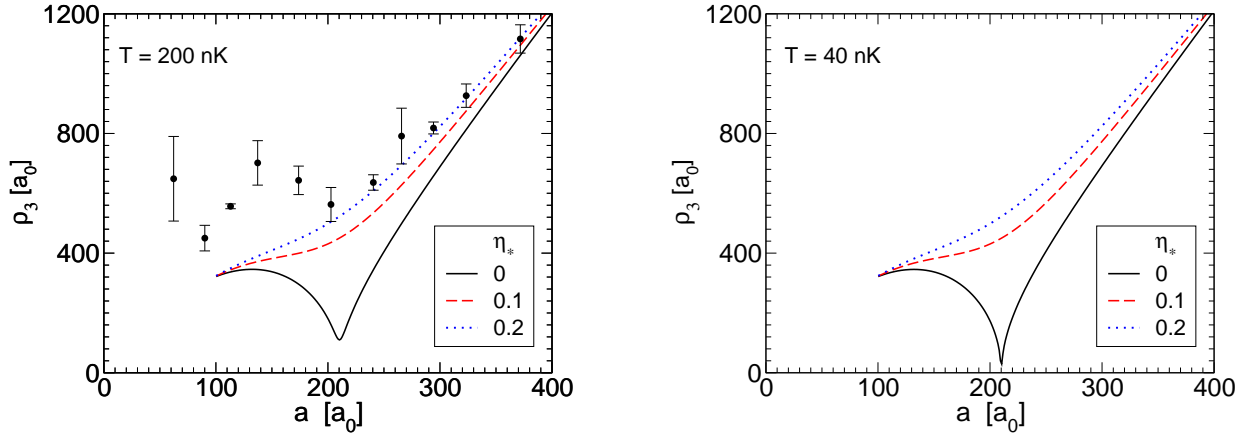


FIG. 9: (Color online) The 3-body recombination length  $\rho_3$  for  $^{133}\text{Cs}$  atoms as a function of  $a$  for  $T = 200$  nK (left panel) and  $T = 40$  nK (right panel). The data points for  $T = 200$  nK are from Ref. [16]. The curves are the universal prediction for three values of  $\eta_*$ : 0 (solid lines), 0.1 (dashed lines), and 0.2 (dotted lines).

Also shown is the Innsbruck data for 200 nK. For  $a < 500 a_0$ , the difference between the predictions at  $T = 0$  and 200 nK is very small. At larger values of  $a$ , the prediction is significantly lower at 200 nK. The prediction for  $T = 200$  nK fits the data much better than the prediction for  $T = 0$ . By comparing Figs. 8 and 10, we can see that increasing  $\eta_*$  and increasing  $T$  both have the effect of decreasing the prediction for  $\rho_3$  for  $a > 500 a_0$

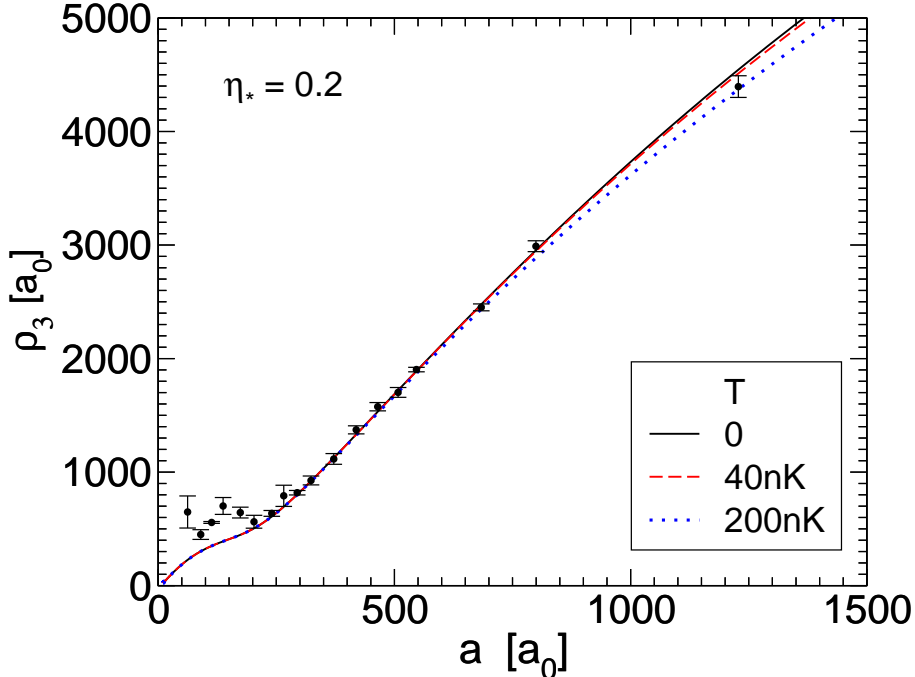


FIG. 10: (Color online) The 3-body recombination length  $\rho_3$  for  $^{133}\text{Cs}$  atoms as a function of  $a$  for  $\eta_* = 0.2$ . The curves are the universal prediction for three values of the temperature:  $T = 0$  (solid line), 40 nK (dashed line), and 200 nK (dotted line). The data points are for  $T = 200$  nK from Ref. [16].

without changing the prediction for smaller values of  $a$ . Thus accurate measurements of the temperature are essential if the data in this region is to be used to determine  $\eta_*$ .

### VIII. COMPARISON WITH PREVIOUS WORK

In this section, we compare our results with previous calculations of the 3-body recombination rate for identical bosons. The previous results include calculations using specific models for the interactions between the atoms as well as calculations based on the universality of atoms with large scattering length.

Esry and D’Incao have calculated the 3-body recombination rate at nonzero temperature by solving the 3-body Schrödinger equation for identical bosons interacting through the simple potential  $V(r) = D/\cosh^2(r/r_0)$  [17, 18]. In Ref. [18], the depth parameter  $D$  was used to vary the scattering length from  $+\infty$  to  $-\infty$  in the region with one 2-body bound state and from  $+\infty$  to  $-\infty$  in the region with two bound states. This range of  $D$  includes three universal regions with large scattering length. The range parameter  $r_0$  determines the two 3-body parameters  $\kappa_*$  and  $\eta_*$  for each of those universal regions. To apply this simple model to the Innsbruck experiment on  $^{133}\text{Cs}$  atoms, Esry and D’Incao tuned  $r_0$  to fit the position of the recombination resonance at  $a = -850 a_0$ . The predicted height of this resonance is larger than that measured by the Innsbruck group. Since  $\eta_*$  is sensitive to the height and width of the resonance, tuning  $r_0$  to get the correct value of  $\kappa_*$  gives too small a value for  $\eta_*$ . Esry and D’Incao also compared the predictions of their model to the

Innsbruck data on  $^{133}\text{Cs}$  atoms with a large positive scattering length. The model does not give a good fit to the data for large positive scattering length. It predicts, for example, a local minimum of the recombination rate for  $a$  near  $1500 a_0$ , which is inconsistent with the data. A better fit to the data for  $a > 0$  could have been obtained by tuning  $r_0$  to fit the measured position of the recombination minimum near  $210 a_0$ .

Massignan and Stoof have calculated the 3-body recombination rate at nonzero temperature by solving the Skorniakov–Ter-Martirosian equation in a scattering model for the lowest hyperfine spin state of  $^{133}\text{Cs}$  atoms [19]. Their scattering model is defined by a 2-body T-matrix element with 5 parameters that models the Feshbach resonance of  $^{133}\text{Cs}$  atoms centered at  $B = -11$  G. The 5 parameters consist of the large background scattering length  $a_{bg} = 1800 a_0$ , the background effective range  $r_{bg}$ , and Feshbach resonance parameters  $B_0$ ,  $\Delta B$ , and  $\Delta\mu$ . The background scattering length  $a_{bg}$  and the Feshbach resonance parameters determine the scattering length  $a(B)$  as a function of the magnetic field  $B$ . The background effective range  $r_{bg}$  could be determined from  $a_{bg}$  and the van der Waals coefficient  $C_6$  for Cs atoms by exploiting the fact that the interatomic potential is  $-C_6/r^6$  at long distances [43, 44]. The resulting estimate is  $r_{bg} \approx +250 a_0$ . However Massignan and Stoof used  $r_{bg}$  as a tuning parameter for 3-body physics. They fit the position of the recombination resonance at  $a = -8500 a_0$  observed by the Innsbruck group by tuning  $r_{bg}$  to the tiny negative value  $-0.27 a_0$ . For  $T = 10$  nK, the prediction of the model for the recombination length  $\rho_3$  at the peak of the resonance is too large by 40%, which is about 4 standard deviations. In the nonuniversal region of small scattering length, the model predicts a minimum in the 3-body recombination rate near  $-150 a_0$  that was not observed in the experiment. For positive scattering length, the model does not give a good quantitative fit to the 200 nK data. It predicts the local minimum to be at  $240 a_0$ , which is a little larger than the observed position  $210(10) a_0$ . At the minimum, the prediction for  $\rho_3$  is less than half the measured value, which is too small by more than 10 standard deviations. At  $a = 1228 a_0$ , their prediction for the recombination length  $\rho_3$  is too large by 10%, which is about 2 standard deviations. Massignan and Stoof could have obtained a better fit to the data for  $a > 0$  by tuning  $r_{bg}$  to fit the measured position of the recombination minimum near  $210 a_0$ .

Lee, Köhler, and Julienne have calculated the 3-body recombination rate at  $T = 0$  using a coupled-channel potential model for the relevant hyperfine spin states of  $^{133}\text{Cs}$  atoms [45]. Their model had 6 fitting parameters: two interchannel coupling parameters that were tuned to fit the position and width of the Feshbach resonance and 4 parameters in a separable interatomic potential that were tuned to fit the background scattering length, the background effective range, and the binding energies of the two shallowest deep dimers [45]. They compared their zero-temperature calculations with the measurements of the Innsbruck group at nonzero temperature. The agreement between their calculation and the Innsbruck data is not very good even at a qualitative level. Their prediction for the magnetic field of the recombination resonance in the  $a < 0$  region is 5.1 G compared with the measured value of 7.4 G [42]. Away from the resonance, their predictions for  $(\rho_3)^4$  are sometimes lower than the 10 nK data by about 2 orders of magnitude. In the  $a > 0$  region, their predictions for  $(\rho_3)^4$  were below the 200 nK data by at least one standard deviation at all points and by many standard deviations at some of the points. Their prediction for the position of the recombination minimum is about  $130 a_0$ , which is much smaller than the observed value  $210(10) a_0$ .

Lee, Köhler, and Julienne have criticized universal approaches to the 3-body recombination as being “incomplete” and they claimed that these approaches “could therefore lead to

unreliable conclusions” [45]. These criticisms were based on misconceptions. In the case of  $^{133}\text{Cs}$  atoms, the two deep dimers that are closest to the threshold have an avoided crossing near the Feshbach resonance at  $-11$  G. Lee, Köhler, and Julienne pointed out that as a consequence the probabilities  $Z_{-1}(B)$  and  $Z_{-2}(B)$  for these deep dimers to consist of atoms in the lowest hyperfine spin state change dramatically with the magnetic field. They concluded incorrectly that  $K_{\text{deep}}(0)$  must depend on  $B$  not only through the scattering length  $a(B)$  but also through the strong  $B$ -dependence of the properties of the deep dimers. It should be noted that no quantitative evidence for this conclusion was given in Ref. [45]. Their conclusion would certainly be true of the exclusive recombination rates into each of the deep dimers. What the authors of Ref. [45] did not appreciate is that the inclusive recombination rate summed over all deep dimers is much less sensitive to details involving short distances, such as level crossings between the deep dimers. The inclusive effects of the deep dimers can be taken into account through the 3-body parameter  $\eta_*$ . Universal approaches are certainly “incomplete” in the sense that, although they can describe the inclusive recombination rate into deep dimers and the exclusive recombination rate into the shallow dimer in the case  $a > 0$ , they cannot describe the exclusive recombination rates into individual deep dimers. However, contrary to the suggestion of Ref. [45], there is no reason to expect universal approaches to lead to “unreliable conclusions” for those recombination rates that they can describe.

In Ref. [45], Lee, Köhler, and Julienne referred to universal approaches to the 3-body problem as “universal fitting procedures”. Assuming that the scattering length is known, the universal approach requires fitting the 3-body parameters  $\kappa_*$  and  $\eta_*$ . The universal approach is very economical in the number of fitting parameters. One price that is paid for this economy is that the 3-body parameters depend sensitively on the details of the 2-body potential. They may be so sensitive that the only practical way to determine them is through experimental measurements of 3-body observables. The model used in Ref. [45] has 6 parameters that were used to fit results from a more accurate representation of the 2-body problem [46]. Three of the parameters are sufficient to reproduce the scattering length  $a(B)$  as a function of the magnetic field. The other 3 were used to fit the background effective range and the binding energies of the two shallowest deep dimers. The authors expected this to be sufficient to calculate the 3-body recombination rate accurately. The large errors in their predictions for the positions of the recombination resonance for  $a < 0$  and the recombination minimum for  $a > 0$  shows that this is not the case. It implies that their model does not correctly predict the physical values of  $\kappa_*$  for these two universal regions. One way to proceed would be to add more and more parameters to the interatomic potential and use them to fit additional 2-body observables. However  $\kappa_*$  and  $\eta_*$  might be too sensitive to the details of interactions at short distances to make this approach practical. An alternative that is motivated by the universal approach is to add 2 parameters to the interatomic potential and use them to tune appropriate 3-body observables in the universal region to their measured values, thus tuning  $\kappa_*$  and  $\eta_*$  close to their physical values.

In Refs. [22–24], the 3-body recombination rate for the case  $a > 0$  has been calculated using simplifying assumptions to neglect some of the universal scaling functions. The starting point in Ref. [22] was an approximation in which only the first term in the expression for  $K^{(0)}(E)$  in Eq. (14), which corresponds to the 3-body channel labelled by  $n = 3$ , was retained. Inserting the universal expression for the S-matrix element  $S_{AD,AAA}^{(J=0,3)}(E)$  in Eq. (19b),

this approximation becomes

$$K^{(0)}(E) \approx \frac{144\sqrt{3}\pi^2}{x^4} \left| s_{23}(x) + \frac{s_{21}(x)s_{13}(x)e^{2i\theta_{*0}}}{1 - s_{11}(x)e^{2i\theta_{*0}}} \right|^2 \frac{\hbar a^4}{m}. \quad (57)$$

This approximation could have been avoided by using Eq. (22) for  $K^{(0)}(E)$  as a starting point instead. The first simplifying assumption of Ref. [22] was to neglect  $s_{11}(x)$  in the denominator. According to the analytic result in Eq. (34a), this function is very small at the threshold:  $|s_{11}(0)| \approx 0.002$ . The assumption of Ref. [22] was that  $|s_{11}(x)|$  remains small for larger values of  $x$ . This assumption has now been verified by our explicit calculation of  $s_{11}(x)$ , which shows that  $|s_{11}(x)| < 0.035$  for  $x < 10$ . With this simplifying assumption, the expression for the recombination rate in Eq. (57) can be reduced to

$$K^{(0)}(E) \approx \frac{144\sqrt{3}\pi^2}{x^4} \left| s_{23}(x)e^{-i\theta_{*0}} + s_{21}(x)s_{13}(x)e^{i\theta_{*0}} \right|^2 \frac{\hbar a^4}{m}. \quad (58)$$

The amplitude inside the absolute value sign can be expressed as a linear combination of  $\cos \theta_{*0}$  and  $\sin \theta_{*0}$  with coefficients that are complex functions of  $x$ . The coefficient of  $\sin \theta_{*0}$  can be made real-valued by multiplying the amplitude by an  $x$ -dependent phase that does not affect the rate. Thus the approximation in Eq. (58) depends on 3 independent real-valued scaling functions. The second simplifying assumption of Ref. [22] was that the coefficients of  $\cos \theta_{*0}$  and  $\sin \theta_{*0}$  were relatively real. This assumption was motivated by the existence of a deep minimum in  $K^{(0)}(E)$  at  $E = 2.1$  mK in the 3-body recombination rate for  $^4\text{He}$  atoms calculated in Ref. [38]. This behavior can be most easily understood if the square of the complex amplitude in Eq. (58) can be approximated by the square of a real amplitude that vanishes at  $E = 2.1$  mK. Given the second simplifying assumption, the approximation in Eq. (58) depends on only two independent scaling functions. In Ref. [22], these two scaling functions were constrained by the requirement that they reproduce the result of Ref. [38] for  $K^{(0)}(E)$  for  $^4\text{He}$  atoms interacting through the HFD-B3-FCI1 potential, which corresponds to  $a = 1.15 a_{*0}$ . By assuming the absence of a near cancellation between the two scaling functions for  $a = 1.15 a_{*0}$ , they obtained predictions for the recombination rate with surprisingly narrow error bands in the region of  $a$  near  $a_{*0}$ . In Ref. [23], Shepard reduced the error bands to a line by using  $K^{(0)}(E)$  for  $^4\text{He}$  atoms interacting through a second potential to determine the two scaling functions separately. In Ref. [24], Platter and Shepard removed the second simplifying assumption of Ref. [22] by using  $K^{(0)}(E)$  for four different  $^4\text{He}$  potentials to determine the three independent real-valued scaling functions in Eq. (58). Their approximation to the universal results for  $K^{(0)}(E)$  is accurate to better than 5%.

In Refs. [22] and [24], the universal scaling functions that were extracted from calculations of 3-body recombination for  $^4\text{He}$  atoms were applied to  $^{133}\text{Cs}$  atoms with  $a > 0$ . The effects of deep dimers on the 3-body recombination rate into the shallow dimer were obtained by making the substitution in Eq. (48) for  $\log a_{*0}$  in the expression for  $K^{(0)}(E)$  in Eq. (58). Since their approach was unable to determine the function  $s_{12}(x)$  that appears in Eq. (53), they approximated the 3-body recombination rate  $K_{\text{deep}}(E)$  into the deep dimer by its value at  $E = 0$ , which is given in Eq. (55b). In Ref. [22], the error bands associated with undetermined universal scaling functions were small for  $a < 300 a_0$  but they widened rapidly as  $a$  increased, so they were unable to obtain a quantitative fit to the Innsbruck data. In Ref. [24], the authors obtained a reasonably good fit to the Innsbruck data for

$a > 200 a_0$  with values of  $\eta_*$  in the range from 0 to 0.01, although their results tended to lie above the highest data point at  $1228 a_0$ . Our definitive universal results give a significantly better fit. There is a qualitative difference in the dependence on  $\eta_*$  between our definitive universal results and the approximation in Ref. [24]. As  $\eta_*$  increases, the definitive universal prediction in the region  $a > 600 a_0$  decreases as shown in Fig. 8, while the approximation in Ref. [24] increases. The difference comes primarily from the approximation of  $K_{\text{deep}}(E)$  by its threshold value in Ref. [24]. As illustrated in Fig. 7, this is a good approximation for  $E < 0.1 E_D$ , but  $K_{\text{deep}}(E)$  decreases rapidly with  $E$  for energies above  $E_D$ . The calculation of the energy dependence of  $K_{\text{deep}}(E)$  was essential for obtaining the excellent fit to the recombination length of  $^{133}\text{Cs}$  atoms with  $\eta_* = 0.2$  that is illustrated in Fig. 8 and the left panel of Fig. 9.

## IX. SUMMARY AND OUTLOOK

In this work, we have calculated the universal scaling functions that determine the 3-body recombination rate for identical bosons as a function of the collision energy<sup>4</sup>. We used the STM equation to calculate the phase shifts for elastic atom-dimer scattering above the breakup threshold for angular momenta up to  $J = 6$ . For  $J \geq 1$ , the contribution  $K^{(J)}(E)$  to the 3-body recombination rate into the shallow dimer is expressed in terms of a real-valued universal scaling function  $f_J(x)$  in Eq. (17). We determined  $f_J(x)$  for each  $J \geq 1$  by fitting the imaginary part of the atom-dimer phase shift. For  $J = 0$ , the contribution  $K^{(0)}(E)$  to the 3-body recombination rate into the shallow dimer is expressed in terms of three complex-valued universal scaling functions  $s_{11}(x)$ ,  $s_{12}(x)$ , and  $s_{22}(x)$  in Eq. (22). We determined these scaling functions by fitting the S-wave atom-dimer phase shift to Efimov's radial law. The parameters in the universal predictions for the 3-body recombination are the scattering length and the 3-body parameter  $a_{*0}$ . We compared our results to previously published calculations of the 3-body recombination rate of  $^4\text{He}$  atoms for angular momenta up to  $J = 3$  [38]. We used the 3-body recombination rate at threshold calculated in Ref. [38] to determine  $a_{*0}$  for  $^4\text{He}$  atoms. We found good quantitative agreement for the 3-body recombination rate  $K^{(J)}(E)$  as a function of energy in the  $J = 0, 1$ , and 2 channels.

Our results can also be applied to atoms with large scattering length that have deep dimers. The deep dimers provide additional 3-body recombination channels and they also have an effect on the 3-body recombination into the shallow dimer. An additional 3-body parameter  $\eta_*$  is necessary to take into account the inclusive effects of the deep dimers. Remarkably, the 3-body recombination rate is completely determined by the same universal scaling functions that apply at  $\eta_* = 0$ . The  $J = 0$  contribution  $K^{(0)}(E)$  to the 3-body recombination rate into the shallow dimer is expressed in terms of the three complex-valued universal scaling functions  $s_{11}(x)$ ,  $s_{12}(x)$ , and  $s_{22}(x)$  in Eq. (52). The  $J \geq 1$  contributions  $K^{(J)}(E)$  are unaffected by the deep dimers and are still given by Eq. (17). The inclusive rate  $K_{\text{deep}}(E)$  for 3-body recombination rate into deep dimers is expressed in terms of the universal scaling functions  $s_{11}(x)$  and  $s_{12}(x)$  in Eq. (53). We compared our results to measurements by the Innsbruck group of the 3-body recombination rate for  $^{133}\text{Cs}$  atoms with a large positive scattering length at a temperature of 200 nK. We set the 3-body parameter  $a_{*0}$  equal to the position of the recombination minimum measured by the Innsbruck group

---

<sup>4</sup> Numerical results for the universal scaling functions can be obtained by contacting any of the authors.

[42]:  $a_{*0} = 210 a_0$ . We then used the 3-body parameter  $\eta_*$  to fit the dependence of the recombination length on  $a$ . We find that  $\eta_* = 0.2$  gives excellent agreement with the experimental results for  $T = 200$  nK in the region  $a > 200 a_0$ . We also found that lowering the temperature would have an observable effect only for  $a > 500 a_0$ .

Our excellent fit to the  $T = 200$  nK data is particularly remarkable considering that it was obtained by using only the scattering length and two adjustable 3-body parameters. The accuracy of this fit presents a challenge to approaches that use more fitting parameters but tune them to fit 2-body observables in addition to the scattering length, as in Ref. [45]. The 3-body parameters  $\kappa_*$  and  $\eta_*$  associated with a given universal region are complicated functions of the 2-body parameters. The 3-body parameters  $\kappa_*$  and  $\eta_*$  may be too sensitive to details at short distances to be determined accurately by fitting a small number of 2-body observables. It is possible that the only practical way to determine them accurately is by tuning them to fit measurements of 3-body observables.

Our universal results for the 3-body recombination rate have a fractional theoretical uncertainty  $r_s/|a|$ , where  $r_s$  is the effective range. Higher accuracy could be obtained by calculating range corrections. It is known how to account systematically for these corrections using an effective field theory for short-range interactions [11, 13]. A first calculation of the range corrections to the recombination rate into the shallow dimer at threshold and an application to  $^4\text{He}$  atoms has already been carried out [41]. In the future, the range corrections should be calculated for the recombination rate as a function of the energy. The range corrections to the recombination rate into deep dimers should also be calculated. The range corrections are particularly important near a recombination minimum. In particular, they can shift the position of the minimum [41]. In the case of Cs atoms, the importance of range corrections near the recombination minimum is further increased by the fact that the minimum is at a scattering length  $210 a_0$  that is not large compared to the effective range.

Our calculations and those in Refs. [18, 19] have been carried out in the Boltzmann region of temperature and density. It would be useful to have universal predictions for lower temperatures where the Bose-Einstein distribution has to be used. In the Boltzmann region, we only need the hyperangular average  $K(E)$  of the 3-body recombination rate, which can be determined from the atom-dimer phase shifts using unitarity. In the Bose-Einstein region, it is necessary to calculate the 3-body recombination rate directly. This requires the calculation of scattering rates with 3 atoms in the initial state. The relevant S-matrix elements are expressed in terms of universal scaling functions  $s_{11}(x)$ ,  $s_{12}(x)$ ,  $s_{1n}(x)$ , and  $s_{2n}(x)$  in Eq. (19b). The scaling functions  $s_{1n}(x)$  and  $s_{2n}(x)$  would have to be calculated for those 3-atom states labelled by  $n = 3, 4, \dots$  that are most important near the 3-atom threshold.

It is also important to calculate the definitive universal predictions for the 3-body recombination rate for negative scattering length. In this case, recombination can occur only into deep dimers. Previous calculations based on the universal approach have used the adiabatic hyperspherical approximation [20] or a resonance approximation [21]. The relevant universal scaling functions can be determined by calculating 3-atom elastic scattering rates near the 3-atom threshold.

## Acknowledgments

This research was supported in part by the Department of Energy under grants DE-FG02-05ER15715 (EB) and DE-FG02-93ER40756 (LP), by the National Science Foundation under



Grant No. PHY-0653312 (LP), the UNEDF SciDAC Collaboration under DOE Grant DE-FC02-07ER41457 (LP), by an Ohio University postdoctoral fellowship (LP), by the DFG through funds provided to SFB/TR 16 (HWH), by the BMBF under grant number 06BN411 (HWH), and by the Korea Research Foundation under grant KRF-2006-612-C00003 (DK).

---

- [1] V. Efimov, Phys. Lett. **33B**, 563 (1970).
- [2] E. Braaten and H.-W. Hammer, Phys. Rept. **428**, 259 (2006).
- [3] E. Braaten and H.-W. Hammer, Annals Phys. **322**, 120 (2007).
- [4] V. N. Efimov, Sov. J. Nucl. Phys. **12**, 589 (1971).
- [5] V. Efimov, Sov. J. Nucl. Phys. **29**, 546 (1979) [Yad. Fiz. **29**, 1058 (1979)].
- [6] E. Nielsen and J.H. Macek, Phys. Rev. Lett. **83**, 1566 (1999).
- [7] B.D. Esry, C.H. Greene, and J.P. Burke, Phys. Rev. Lett. **83**, 1751 (1999).
- [8] P. F. Bedaque, E. Braaten and H.-W. Hammer, Phys. Rev. Lett. **85**, 908 (2000).
- [9] V. Efimov, Phys. Rev. C **44**, 2303 (1991).
- [10] V. Efimov, Phys. Rev. C **47**, 1876 (1993).
- [11] H.-W. Hammer and T. Mehen, Phys. Lett. B **516**, 353 (2001).
- [12] P. F. Bedaque, G. Rupak, H. W. Griesshammer and H.-W. Hammer, Nucl. Phys. A **714**, 589 (2003).
- [13] L. Platter and D. R. Phillips, Few Body Syst. **40**, 35 (2006).
- [14] E. Braaten, H.-W. Hammer and M. Kusunoki, Phys. Rev. A **67**, 022505 (2003).
- [15] E. Braaten and H.-W. Hammer, Phys. Rev. A **70**, 042706 (2004).
- [16] T. Kraemer, M. Mark, P. Waldburger, J.G. Danzl, C. Chin, B. Engeser, A.D. Lange, K. Pilch, A. Jaakkola, H.-C. Nägerl, and R. Grimm, Nature **440**, 315 (2006).
- [17] J.P. D’Incao, H. Suno, and B. D. Esry, Phys. Rev. Lett. **93**, 123201 (2004).
- [18] J.P. D’Incao and B. D. Esry, arXiv:cond-mat/0703269.
- [19] P. Massignan and H.T.C. Stoof, arXiv:cond-mat/0702462.
- [20] S. Jonsell, Europhys. Lett. **76**, 8 (2006).
- [21] M.T. Yamashita, T. Frederico, and L. Tomio, Phys. Lett. A **363**, 468 (2007).
- [22] E. Braaten, D. Kang and L. Platter, Phys. Rev. A **75**, 052714 (2007).
- [23] J. R. Shepard, Phys. Rev. A **75**, 062713 (2007).
- [24] L. Platter and J. R. Shepard, arXiv:0711.1908 [cond-mat.other].
- [25] E. Braaten and H.-W. Hammer, Phys. Rev. A **75**, 052710 (2007).
- [26] B.D. Esry, C.H. Greene, and H. Suno, Phys. Rev. A **65**, 010705 (2001).
- [27] J.H. Macek, S. Ovchinnikov, and G. Gasaneo, Phys. Rev. A **72**, 032709 (2005).
- [28] J.H. Macek, S. Ovchinnikov, and G. Gasaneo, Phys. Rev. A **73**, 032704 (2006).
- [29] D. Petrov, talk at the Workshop on Strongly Interacting Quantum Gases, Ohio State University, April 2005.
- [30] G.V. Skorniakov and K.A. Ter-Martirosian, Sov. Phys. JETP **4**, 648 (1957) [J. Exptl. Theoret. Phys. (U.S.S.R.) **31**, 775 (1956)].
- [31] P. F. Bedaque, H.-W. Hammer and U. van Kolck, Phys. Rev. Lett. **82**, 463 (1999).
- [32] P. F. Bedaque, H.-W. Hammer and U. van Kolck, Nucl. Phys. A **646**, 444 (1999).
- [33] H.-W. Hammer and T. Mehen, Nucl. Phys. A **690**, 535 (2001).
- [34] H. W. Griesshammer, Nucl. Phys. A **760**, 110 (2005).
- [35] E. Braaten and H.-W. Hammer, Phys. Rev. A **67**, 042706 (2003).

- [36] V. Roudnev and S. Yakovlev, Chem. Phys. Lett. **328**, 97 (2000).
- [37] V. Roudnev, Chem. Phys. Lett. **367**, 95 (2003).
- [38] H. Suno, B.D. Esry, C.H. Greene, and J.P. Burke, Phys. Rev. A **65**, 042725 (2002).
- [39] R.A. Aziz, A.R. Janzen, and M.R. Moldover, Phys. Rev. Lett. **74**, 1586 (1995).
- [40] B.D. Esry and H. Suno, private communication.
- [41] H.-W. Hammer, T. A. Lahde and L. Platter, Phys. Rev. A **75**, 032715 (2007).
- [42] H.-C. Nägerl et al., Proceedings of ICAP-2006 (Innsbruck), arXiv:cond-mat/0611629.
- [43] B. Gao, Phys. Rev. A **58**, 4222 (1998).
- [44] V.V Flambaum, G.F. Gribakin, and C. Harabati, Phys. Rev. A **59**, 1998 (1999).
- [45] M.D. Lee, T. Köhler and P.S. Julienne Phys. Rev. A **76**, 012720 (2007).
- [46] C. Chin, V. Vuletic, A. J. Kerman, S. Chu, E. Tiesinga, P. J. Leo, and C. J. Williams, Phys. Rev. A **70**, 032701 (2004).